Table 1 Association of the *BIM* deletion polymorphism with clinical resistance to imatinib in subjects with CML

	No *BIM* deletion polymorphism % (*n*)	*BIM* deletion polymorphism % (*n*)	
Singaporean and Malaysian cohort (*n* = 138)			
Sensitive	51 (64)	33 (5)	OR = 2.73 (95% CI 0.87–8.57)
Resistant	49 (59)	67 (10)	*P* = 0.09
Japanese cohort (*n* = 65)			
Sensitive	43 (23)	17 (2)	OR = 3.52 (95% CI 0.69–18.00)
Resistant	57 (30)	83 (10)	*P* = 0.13
Combined cohorts OR (*n* = 203)			**OR = 2.94 (95% CI 1.17–7.43) *P* = 0.02**

Subjects with newly diagnosed chronic phase CML were analyzed according to their cohorts of origin (Singaporean and Malaysian or Japanese) and divided into those with and those without the *BIM* deletion polymorphism. Individuals were then classified as resistant ('suboptimal response' or 'failure' per ELN criteria) or sensitive ('optimal response' per ELN criteria) to imatinib. Statistical analysis testing for the association between the *BIM* deletion polymorphism and clinical resistance to imatinib was carried out using logistic regression on the individual cohort tables adjusting for any effects of age differences between groups with and without the *BIM* deletion polymorphism (**Supplementary Table 9**). The unadjusted odds ratio (OR) was 2.85 (*P* = 0.02, 95% CI 1.15–7.08). The statistics for the combined cohorts are shown in bold for visualization purposes and to distinguish these results from those of each individual cohort.

By comparison, we found no significant differences between the two groups with respect to other potential prognostic or confounding factors, including median time from diagnosis to initiation of imatinib treatment, Sokal score at diagnosis or prior treatment with interferon (**Supplementary Table 9**). We also noted that the majority of resistant subjects with the polymorphism subsequently did not respond to second-generation TKI therapy (**Supplementary Table 10**), a finding that is in line with the intrinsic resistance we observed in the cell lines.

TKI resistance in CML is most commonly associated with the acquisition of somatic mutations in the *BCR-ABL1* kinase domain, which can be found in up to 50% of resistant individuals in the chronic phase of disease[28]. However, because the deletion polymorphism is germline and is sufficient to cause intrinsic TKI resistance *in vitro* (**Fig. 3**), we predicted that such individuals would be resistant even in the absence of a kinase-domain mutation. Accordingly, we divided the subjects into the following three clinical groups: resistant without a *BCR-ABL1* mutation (group 1), resistant with a *BCR-ABL1* mutation (group 2) or sensitive (group 3). We found that individuals with the polymorphism, compared to those without, were more likely to be in group 1 than in groups 2 and 3 combined (odds ratio = 1.90, 95% CI 1.08–4.35) (**Supplementary Table 11**). These data provide a second clinical validation of our hypothesis.

The *BIM* deletion as a biomarker in EGFR NSCLC

We next validated the role of the *BIM* polymorphism in another kinase-driven cancer, EGFR NSCLC, in which sensitizing mutations in EGFR predict high response rates in individuals treated with EGFR inhibitors[29,30] and in which BIM expression is required for TKI sensitivity[11–13]. An additional and relevant aspect of this cancer is that it is particularly common in East Asian countries, where activating *EGFR* mutations can be found in up to 50% of NSCLCs (compared to 15% in the western countries[4]) and are enriched for among female East Asian nonsmokers[31–33].

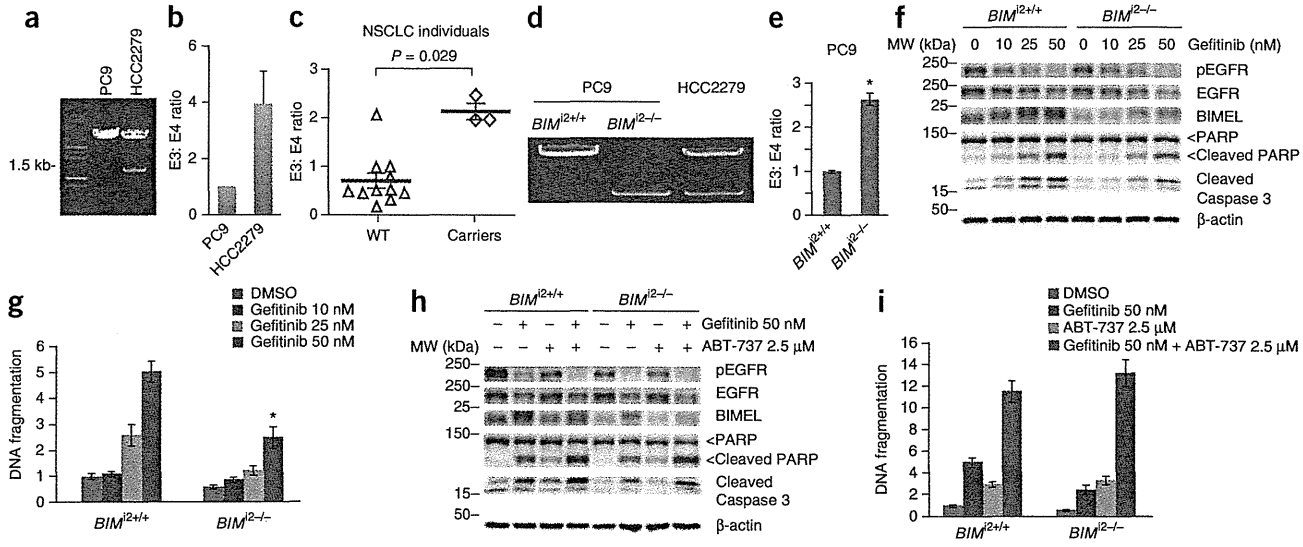

Figure 4 The *BIM* deletion polymorphism is sufficient to cause intrinsic TKI resistance in EGFR NSCLC cell lines. (**a**) An agarose gel of the PCR products, using the method described in **Figure 1c** to detect the polymorphism in HCC2279 cells. (**b**) Ratio of exon-3– to exon-4–containing transcripts in NSCLC cell lines with (HCC2279) and without (PC9) the deletion polymorphism. Data are mean ± s.e.m. (**c**) Peripheral blood mononuclear cells were obtained from subjects with EGFR NSCLC with and without the deletion and were analyzed for the ratio of exon 3 to exon 4 transcripts using qPCR, as described in **Figure 2d**. (**d**) An agarose gel of the PCR products, using the method described in **Figure 1c** to detect the polymorphism in genome-edited PC9 cell lines, with HCC2279 cells being used as a control. Clones that were negative for the deletion polymorphism (PC9-*BIM*$^{i2+/+}$), as well as those homozygous (PC9-*BIM*$^{i2-/-}$) for it, were isolated. (**e**) The ratio of exon 3 to exon 4 transcripts as measured by qPCR in PC9-*BIM*$^{i2+/+}$ and PC9-*BIM*$^{i2-/-}$cells. Data are mean ± s.e.m. *P = 0.0011 (Student's t test). (**f**) Western blots of cell lysates from PC9-*BIM*$^{i2+/+}$ and PC9-*BIM*$^{i2-/-}$ cells after treatment with increasing concentrations of gefitinib. (**g**) Relative apoptotic cell death, using the method described in **Figure 3f**, of PC9-*BIM*$^{i2+/+}$ and PC9-*BIM*$^{i2-/-}$ cells treated using DMSO or different concentrations of gefitinib, as indicated. Data are mean ± s.e.m. *P = 0.0009 (Student's t test). (**h**) Western blot of cell lysates from PC9-*BIM*$^{i2+/+}$ and PC9-*BIM*$^{i2-/-}$ cells treated with gefitinib, ABT-737 or both. (**i**) Relative apoptotic cell death, using the method described in **Figure 3f**, for cells treated as in **h**. Data are mean ± s.e.m.

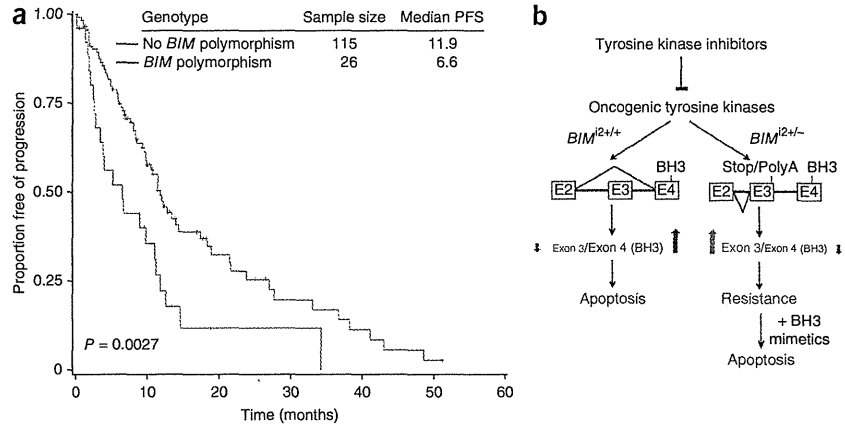

Figure 5 The *BIM* deletion polymorphism predicts shorter PFS in individuals with *EGFR*-mutant NSCLC treated with EGFR TKI therapy. (**a**) The presence or absence of the *BIM* deletion polymorphism was determined in 141 subjects with NSCLC from Singapore and Japan who were known to have activating mutations in EGFR and who received TKI therapy. The PFS for each group was estimated using the Kaplan-Meier method. (**b**) Schematic depicting the mechanism by which the *BIM* deletion polymorphism causes TKI resistance. After TKI exposure, wild-type cells that do not contain the deletion ($BIM^{i2+/+}$) preferentially upregulate expression of exon-4–containing (and, therefore, BH3-encoding) *BIM* transcripts that are capable of activating apoptosis (the red line corresponds to the 2,903-kb deleted region). In contrast, cells that harbor the deletion ($BIM^{i2+/-}$) favor the splicing and expression of exon-3–containing transcripts that do not encode the BH3 domain. The generation of exon-3–containing isoforms occurs at the expense of exon-4–containing isoforms, and as a result, the decreased concentrations of BH3-containing BIM protein isoforms render cells relatively TKI resistant. In these cells, restoration of TKI sensitivity can be brought about by the addition of BH3-mimetic drugs.

First we searched for NSCLC cell lines that harbored TKI-sensitizing *EGFR* mutations but were inexplicably TKI resistant (defined as lacking any of the known secondary-resistance–conferring mutations). We identified one such line, HCC2279, which notably fails to activate apoptosis despite effective EGFR inhibition[34,35]. We confirmed the presence of the *BIM* deletion polymorphism in the HCC2779 cells (**Fig. 4a**) and determined the effects of the deletion polymorphism on BIM function. The deletion resulted in greater expression of exon-3–containing compared to exon-4–containing (and, hence, BH3-containing) BIM isoforms compared to cells without the polymorphism (**Fig. 4b**). Notably, primary peripheral blood mononuclear cells from subjects with EGFR NSCLC, and with or without the deletion polymorphism, showed this same phenomenon (**Fig. 4c**). HCC2279 cells also had decreased induction of exon-4–containing transcripts and BIMEL protein after TKI exposure, as well as impaired activation of apoptotic signaling, as measured by poly (ADP-ribose) polymerase (PARP) cleavage (**Supplementary Fig. 4a,b**). Consistent with the notion that TKI resistance is a result of decreased concentrations of BH3-containing BIM protein, the addition of the BH3-mimetic drug ABT-737 enhanced TKI-induced apoptotic signaling and cell death (**Supplementary Fig. 4c,d**). To confirm that the polymorphism was sufficient to cause TKI resistance in EGFR NSCLC, we introduced it into TKI-sensitive PC9 cells (**Fig. 4d**). Analogous to our findings in K562-$BIM^{i2-/-}$ cells (**Fig. 3**), we found that, compared to PC9-$BIM^{i2+/+}$ cells, PC9-$BIM^{i2-/-}$ cells had decreased expression of exon-4–containing and BH3-containing BIM transcripts and protein, respectively, were intrinsically TKI resistant and were re-sensitized to TKIs by ABT-737 (**Fig. 4e–i**).

Next, we asked whether the deletion correlated with the duration of response to EGFR TKIs in subjects with NSCLC with activating *EGFR* mutations. Individuals with or without the deletion polymorphism did not differ with respect to known prognostic factors, including stage (as more than 85% of the subjects were stage IV) (**Supplementary Table 12**). Nevertheless, the presence of the polymorphism was predictive of a significantly shorter PFS, with a median PFS of 6.6 months in individuals with the polymorphism compared to 11.9 months for those without it ($n = 141$, $P = 0.0027$) (**Fig. 5a**). In multivariate analyses using the Cox regression model, only the deletion polymorphism (hazard ratio = 2.08, 95% CI 1.29–3.38, $P = 0.0028$) and the presence of the TKI-resistant exon 20 mutation (hazard ratio = 5.11, 95% CI 1.43–18.31, $P = 0.012$)[36,37] emerged as independent prognostic factors for shorter PFS.

DISCUSSION

Our findings demonstrate the principle that, although cancers should be classified according to their somatically acquired driver mutations, germline polymorphisms can directly modulate the responses of such cancers to targeted therapies and can strongly influence clinical outcomes. Notably, we show how a common *BIM* deletion polymorphism contributes to the heterogeneity of responses seen among molecularly defined patients with cancer who are treated with targeted therapies. Our data also highlight how a single germline polymorphism can strongly affect clinical outcomes in different cancers that share a common biology and probably reflect the central role of BIM in mediating TKI sensitivity in these diseases[8,11,13]. We anticipate that the list of cancers in which the *BIM* polymorphism influences TKI responses will expand to include others that also depend on BIM expression for TKI sensitivity[38–40].

The *BIM* polymorphism is found only in individuals of East Asian descent. It is therefore interesting to note that in CML, a higher rate of incomplete cytogenetic responses to imatinib has been reported among individuals in East Asia (~50%) compared to individuals in Europe and North America (26%)[41]. To assess the relative contribution of the deletion polymorphism to these ethnic differences, we estimated that the polymorphism underlies resistance in ~21% of East Asian patients (for the population attributable fraction, see the Online Methods). This might explain, in part, the differences in complete cytogenetic response rates observed between these two world populations.

As a germline biomarker for TKI resistance, the *BIM* polymorphism also offers several advantages over biomarkers comprising acquired mutations. First, the *BIM* polymorphism can be used at the time of initial presentation to predict which individuals are at an increased risk of developing TKI resistance, and second, the assessment of an individual's polymorphism status does not require an analysis of tumor-specific DNA. The former characteristic offers the potential for preventing the emergence of TKI resistance by therapeutic means (for example, treatment with a BH3-mimetic drug at the time of initial presentation or at the first sign of resistance), whereas the latter characteristic is particularly advantageous in solid tumor situations, as in EGFR NSCLC, when a second biopsy for tumor-specific tissue usually necessitates an invasive procedure. Although recent work has highlighted the value of *BIM* RNA levels in tumors before treatment in predicting TKI responsiveness[42], our discovery emphasizes the

importance of biomarkers that can also predict the induction of functional isoforms of BIM after TKI exposure.

By elucidating the effects of the deletion polymorphism on BIM function, we also were able to describe a previously unknown splicing mechanism by which the polymorphism contributes to drug resistance in CML and EGFR NSCLC (**Fig. 5b**). Thus, in showing that resistance is caused by impaired expression of BH3-containing BIM isoforms, we confirmed that pharmacologic restoration of BIM function could overcome this particular form of TKI resistance in both cancers. Our findings also support the increasingly recognized role of alterations in the splicing pattern of genes in human disease[43,44] and provide a new example of an inherited mutation that contributes to resistance against targeted cancer therapies. However, we note that although the presence of the deletion polymorphism is strongly associated with clinical TKI resistance and shorter PFS, other genetic factors, both acquired and inherited, will probably dictate the final response to TKI therapy in any individual patient. Indeed, several other mechanisms of EGFR-independent resistance have been described, including upregulated hepatocyte growth factor–dependent signaling[45], nuclear factor κ-light-chain-enhancer of activated B cells (NF-κB)-dependent signaling[46] and v-Ki-ras2 Kirsten rat sarcoma viral oncogene homolog (KRAS) mutations[47]. It will therefore be crucial to determine how these factors interact with each other to contribute to TKI resistance, which, given the relatively low incidence of each individual contributor, will require larger prospective studies.

Clinical resistance to TKIs has been commonly classified as being primary or secondary, with the latter defined as occurring in individuals who experienced an initial response to TKI therapy and then later developed resistance. It is also assumed that secondary resistance is mediated by acquired somatic mutation(s) that emerge under the selective pressure of TKI therapy, whereas intrinsic mechanisms of resistance (including germline polymorphisms) are more likely to present with primary resistance and a lack of any upfront response. This line of reasoning is based on the assumption that resistance-conferring germline polymorphisms result in absolute as opposed to relative TKI resistance. However, by creating both CML and EGFR NSCLC cells with the deletion, we show that the *BIM* polymorphism results in relative TKI resistance. This finding is consistent with cancer cells being sensitive to small changes in BIM protein concentrations[8,48] and with BIM protein concentrations exerting a dose-dependent effect on apoptosis and on the degree of TKI resistance[8]. Accordingly, we expected to see some degree of response in TKI-treated subjects harboring the polymorphism, which we indeed confirmed in the setting of both CML and EGFR NSCLC.

Although our data focus on the effect of polymorphisms on therapeutic responses, it is possible that human polymorphisms also account for heterogeneity among other aspects of cancer biology. Unlike the *BIM* deletion, these other polymorphisms could conceivably result in enhanced therapeutic responses or could even cooperate with driver mutations to accelerate or delay cancer progression. As we have shown, a mechanistic understanding of how such polymorphisms affect gene function may lead to improved management of patients with cancer with respect to prognostication and therapy. In the case of TKI resistance in individuals with the *BIM* polymorphism, the addition of BH3 mimetics to the standard TKI therapy may allow for personalized treatment to overcome resistance or even to prevent its emergence. Finally, although the ethnic segregation of the polymorphism is in itself interesting, the greater importance of our findings may be that it is prototypic of other polymorphisms, yet to be discovered, that account for intrinsic drug resistance in different world populations.

METHODS

Methods and any associated references are available in the online version of the paper at http://www.nature.com/naturemedicine/.

Accession codes. The sequencing data have been submitted to the NCBI Gene Expression Omnibus (http://www.ncbi.nlm.nih.gov/geo/) under accession number GSE28303 (clinical samples) and GSE26954 (K562), and were analyzed as described in the Online Methods.

Note: Supplementary information is available on the Nature Medicine website.

ACKNOWLEDGMENTS

This study was supported by grants from the National Medical Research Council of Singapore and the Biomedical Research Council (BMRC) of the Agency for Science, Technology and Research (A*STAR), Singapore. Additional support was also provided by the Genome Institute of Singapore internal research funds from the BMRC and the Department of Clinical Research, Singapore General Hospital. We are grateful for insightful conversations regarding this study with G. Bourque, M. Garcia-Blanco, E. Liu, X. Roca, S. Rosen, S. Shenolikar, D. Virshup and M. Voorhoeve. We thank C.-L. Wei and H. Thoreau for management of the sequencing platform, S.T. Leong, S.C. Neo and P.S. Choi for sequencing, J. Chen and C.S. Chan for help in data processing, H.P. Lim, Y.Y. Sia and Y.H. Choy for PCR validation and A. Lim and T.H. Lim for assistance in the fluorescence *in situ* hybridization (FISH) analysis. We also thank M. Garcia-Blanco (Duke University), K. Itahana (Duke-NUS), A. Vazquez (Institut National de la Santé et de la Recherche Médicale U.1014, Villejuif, France and Université Paris-Sud, Paris, France) and P. Koeffler (Cedars-Sinai Medical Center, Los Angeles, California, USA and Cancer Science Institute of Singapore, Singapore) for the kind gifts of the pl-12 vector, pcDNA3-FLAG3 plasmid, BIM expression vectors and NSCLC cell lines, respectively. Finally, we are grateful to the patients and physicians at the Department of Haematology, Singapore General Hospital, the Department of Hematology-Oncology, Akita University Hospital, Japan, the Toho University Omori Medical Center, Japan, the Aichi Cancer Center, Japan, the National University Cancer Institute, National University Health System, Singapore, National Cancer Centre, Singapore and the University of Malaya Medical Centre, Kuala Lumpur, Malaysia who contributed patient material.

AUTHOR CONTRIBUTIONS

K.P.N. and A.M.H. performed data analyses, generated the list of structural variations, validated the paired-end ditag data and wrote the first draft of the manuscript. C.T.H.C. provided CML clinical input and generated and analyzed the clinical data in **Table 1**. W.C.J. and T.K.K. devised and performed the experiments in **Figures 2–4**. C.-T.C. performed the experiments in **Figures 3** and **4**. J.W.J.H. performed FISH and PCR analysis on patient and normal control samples. A.S.M.T. and Y.F. constructed DNA-PET libraries for high-throughput sequencing. P.N.A., W.H.L. and W.-K.S. developed the bioinformatics pipeline for the DNA-PET analysis, N.N. contributed to the pipeline development, and X.Y.W. developed the copy number analysis. W.T.P. ran the bioinformatics pipeline. V.K. and A.T. performed *BIM* deletion screening in the HapMap samples, and A.T. performed the population-level genetic statistical analysis. X.R. managed the high-throughput sequencing, and A.S. managed the bioinformatics infrastructure. C.T.H.C., N.T., K.S., A.L.A., H.T.M., G.F.H., L.Y.Y., L.P.K., B.C., V.S.N., W.J.C., H.T., L.C.L. and Y.T.G. provided samples from patients with CML, as well as clinical data from the same patients. M.M.N. and T.Y.W. provided samples from normal individuals. K.P.N., J.W.J.H. and W.C.J. analyzed CML samples for the *BIM* deletion polymorphism. J.C.A. Jr. performed the statistical analysis of the CML clinical data. V.C.-R. performed and interpreted FISH data and provided scientific advice. S.S. compiled the clinical data and, together with J.C.A. Jr., performed the statistical analyses for **Figure 5a**. K.P.N., J.W.J.H., S.Z., D.P., P.T. and M.S. analyzed samples for *EGFR* mutations and the *BIM* deletion polymorphism. J.-E.S., M.-K.A., N.-M.C., Q.-S.N., D.S.W.T., K.I., Y.Y., H.M., E.H.T., R.A.S., T.M.C. and W.-T.L. provided samples from subjects with EGFR NSCLC, as well as the accompanying clinical data. Y.R. and S.T.O. designed and directed the study and analyzed data. S.T.O. wrote the final draft of the manuscript, which was reviewed by K.P.N., A.M.H., C.T.H.C., W.C.J., T.K.K., W.-T.L. and Y.R.

COMPETING FINANCIAL INTERESTS

The authors declare competing financial interests: details accompany the full-text HTML version of the paper at http://www.nature.com/naturemedicine/.

Published online at http://www.nature.com/naturemedicine/.
Reprints and permissions information is available online at http://www.nature.com/reprints/index.html.

1. Jänne, P.A., Gray, N. & Settleman, J. Factors underlying sensitivity of cancers to small-molecule kinase inhibitors. *Nat. Rev. Drug Discov.* **8**, 709–723 (2009).
2. Carella, A.M. *et al.* New insights in biology and current therapeutic options for patients with chronic myelogenous leukemia. *Haematologica* **82**, 478–495 (1997).
3. Schiller, J.H. *et al.* Comparison of four chemotherapy regimens for advanced non–small-cell lung cancer. *N. Engl. J. Med.* **346**, 92–98 (2002).
4. Keedy, V.L. *et al.* American Society of Clinical Oncology provisional clinical opinion: epidermal growth factor receptor (EGFR) mutation testing for patients with advanced non–small-cell lung cancer considering first-line EGFR tyrosine kinase inhibitor therapy. *J. Clin. Oncol.* **29**, 2121–2127 (2011).
5. Baccarani, M. *et al.* Chronic myeloid leukemia: an update of concepts and management recommendations of European LeukemiaNet. *J. Clin. Oncol.* **27**, 6041–6051 (2009).
6. Wang, L., McLeod, H.L. & Weinshilboum, R.M. Genomics and drug response. *N. Engl. J. Med.* **364**, 1144–1153 (2011).
7. Youle, R.J. & Strasser, A. The BCL-2 protein family: opposing activities that mediate cell death. *Nat. Rev. Mol. Cell Biol.* **9**, 47–59 (2008).
8. Kuroda, J. *et al.* Bim and Bad mediate imatinib-induced killing of Bcr/Abl$^+$ leukemic cells, and resistance due to their loss is overcome by a BH3 mimetic. *Proc. Natl. Acad. Sci. USA* **103**, 14907–14912 (2006).
9. Aichberger, K.J. *et al.* Low-level expression of proapoptotic Bcl-2-interacting mediator in leukemic cells in patients with chronic myeloid leukemia: role of BCR/ABL, characterization of underlying signaling pathways, and reexpression by novel pharmacologic compounds. *Cancer Res.* **65**, 9436–9444 (2005).
10. Kuribara, R. *et al.* Roles of Bim in apoptosis of normal and Bcr-Abl–expressing hematopoietic progenitors. *Mol. Cell. Biol.* **24**, 6172–6183 (2004).
11. Cragg, M.S., Kuroda, J., Puthalakath, H., Huang, D.C. & Strasser, A. Gefitinib-induced killing of NSCLC cell lines expressing mutant EGFR requires BIM and can be enhanced by BH3 mimetics. *PLoS Med.* **4**, 1681–1689 (2007).
12. Gong, Y. *et al.* Induction of BIM is essential for apoptosis triggered by EGFR kinase inhibitors in mutant EGFR-dependent lung adenocarcinomas. *PLoS Med.* **4**, e294 (2007).
13. Costa, D.B. *et al.* BIM mediates EGFR tyrosine kinase inhibitor-induced apoptosis in lung cancers with oncogenic EGFR mutations. *PLoS Med* **4**, 1669–1679 (2007).
14. Fullwood, M.J., Wei, C.L., Liu, E.T. & Ruan, Y. Next-generation DNA sequencing of paired-end tags (PET) for transcriptome and genome analyses. *Genome Res.* **19**, 521–532 (2009).
15. Hillmer, A.M. *et al.* Comprehensive long-span paired-end-tag mapping reveals characteristic patterns of structural variations in epithelial cancer genomes. *Genome Res.* **21**, 665–675 (2011).
16. Liu, J.W., Chandra, D., Tang, S.H., Chopra, D. & Tang, D.G. Identification and characterization of Bimgamma, a novel proapoptotic BH3-only splice variant of Bim. *Cancer Res.* **62**, 2976–2981 (2002).
17. Adachi, M., Zhao, X. & Imai, K. Nomenclature of dynein light chain-linked BH3-only protein Bim isoforms. *Cell Death Differ.* **12**, 192–193 (2005).
18. Ladd, A.N. & Cooper, T.A. Finding signals that regulate alternative splicing in the post-genomic era. *Genome Biol.* **3**, reviews0008 (2002).
19. Carstens, R.P., McKeehan, W.L. & Garcia-Blanco, M.A. An intronic sequence element mediates both activation and repression of rat fibroblast growth factor receptor 2 pre-mRNA splicing. *Mol. Cell. Biol.* **18**, 2205–2217 (1998).
20. Cheng, E.H. *et al.* BCL-2, BCL-X(L) sequester BH3 domain-only molecules preventing BAX- and BAK-mediated mitochondrial apoptosis. *Mol. Cell* **8**, 705–711 (2001).
21. Huang, D.C. & Strasser, A. BH3-only proteins-essential initiators of apoptotic cell death. *Cell* **103**, 839–842 (2000).
22. Kubonishi, I. & Miyoshi, I. Establishment of a Ph1 chromosome-positive cell line from chronic myelogenous leukemia in blast crisis. *Int. J. Cell Cloning* **1**, 105–117 (1983).
23. Mahon, F.X. *et al.* Selection and characterization of BCR-ABL positive cell lines with differential sensitivity to the tyrosine kinase inhibitor STI571: diverse mechanisms of resistance. *Blood* **96**, 1070–1079 (2000).
24. Deininger, M.W., Goldman, J.M., Lydon, N. & Melo, J.V. The tyrosine kinase inhibitor CGP57148B selectively inhibits the growth of BCR-ABL–positive cells. *Blood* **90**, 3691–3698 (1997).
25. Shah, N.P. *et al.* Transient potent BCR-ABL inhibition is sufficient to commit chronic myeloid leukemia cells irreversibly to apoptosis. *Cancer Cell* **14**, 485–493 (2008).
26. Ly, C., Arechiga, A.F., Melo, J.V., Walsh, C.M. & Ong, S.T. Bcr-Abl kinase modulates the translation regulators ribosomal protein S6 and 4E–BP1 in chronic myelogenous leukemia cells via the mammalian target of rapamycin. *Cancer Res.* **63**, 5716–5722 (2003).
27. Cragg, M.S., Harris, C., Strasser, A. & Scott, C.L. Unleashing the power of inhibitors of oncogenic kinases through BH3 mimetics. *Nat. Rev. Cancer* **9**, 321–326 (2009).
28. La Rosée, P. & Hochhaus, A. Resistance to imatinib in chronic myelogenous leukemia: mechanisms and clinical implications. *Curr. Hematol. Malig. Rep.* **3**, 72–79 (2008).
29. Paez, J.G. *et al.* EGFR mutations in lung cancer: correlation with clinical response to gefitinib therapy. *Science* **304**, 1497–1500 (2004).
30. Lynch, T.J. *et al.* Activating mutations in the epidermal growth factor receptor underlying responsiveness of non–small-cell lung cancer to gefitinib. *N. Engl. J. Med.* **350**, 2129–2139 (2004).
31. Shepherd, F.A. *et al.* Erlotinib in previously treated non–small-cell lung cancer. *N. Engl. J. Med.* **353**, 123–132 (2005).
32. Kim, E.S. *et al.* Gefitinib versus docetaxel in previously treated non–small-cell lung cancer (INTEREST): a randomised phase III trial. *Lancet* **372**, 1809–1818 (2008).
33. Park, K. & Goto, K. A review of the benefit-risk profile of gefitinib in Asian patients with advanced non-small-cell lung cancer. *Curr. Med. Res. Opin.* **22**, 561–573 (2006).
34. Lu, Y., Liang, K., Li, X. & Fan, Z. Responses of cancer cells with wild-type or tyrosine kinase domain–mutated epidermal growth factor receptor (EGFR) to EGFR-targeted therapy are linked to downregulation of hypoxia-inducible factor-1α. *Mol. Cancer* **6**, 63 (2007).
35. Machida, K. *et al.* Characterizing tyrosine phosphorylation signaling in lung cancer using SH2 profiling. *PLoS ONE* **5**, e13470 (2010).
36. Wu, J.Y. *et al.* Lung cancer with epidermal growth factor receptor exon 20 mutations is associated with poor gefitinib treatment response. *Clin. Cancer Res.* **14**, 4877–4882 (2008).
37. Sasaki, H. *et al.* EGFR exon 20 insertion mutation in Japanese lung cancer. *Lung Cancer* **58**, 324–328 (2007).
38. Gordon, P.M. & Fisher, D.E. Role for the proapoptotic factor BIM in mediating imatinib-induced apoptosis in a c-KIT-dependent gastrointestinal stromal tumor cell line. *J. Biol. Chem.* **285**, 14109–14114 (2010).
39. Will, B. *et al.* Apoptosis induced by JAK2 inhibition is mediated by Bim and enhanced by the BH3 mimetic ABT-737 in JAK2 mutant human erythroid cells. *Blood* **115**, 2901–2909 (2010).
40. Soda, M. *et al.* Identification of the transforming EML4-ALK fusion gene in non–small-cell lung cancer. *Nature* **448**, 561–566 (2007).
41. Au, W.Y. *et al.* Chronic myeloid leukemia in Asia. *Int. J. Hematol.* **89**, 14–23 (2009).
42. Faber, A. *et al.* BIM expression in treatment naive cancers predicts responsiveness to kinase inhibitors. *Cancer Discov.* **1**, 352–365 (2011).
43. Cartegni, L., Chew, S.L. & Krainer, A.R. Listening to silence and understanding nonsense: exonic mutations that affect splicing. *Nat. Rev. Genet.* **3**, 285–298 (2002).
44. López-Bigas, N., Audit, B., Ouzounis, C., Parra, G. & Guigo, R. Are splicing mutations the most frequent cause of hereditary disease? *FEBS Lett.* **579**, 1900–1903 (2005).
45. Yano, S. *et al.* Hepatocyte growth factor induces gefitinib resistance of lung adenocarcinoma with epidermal growth factor receptor–activating mutations. *Cancer Res.* **68**, 9479–9487 (2008).
46. Bivona, T.G. *et al.* FAS and NF-κB signalling modulate dependence of lung cancers on mutant EGFR. *Nature* **471**, 523–526 (2011).
47. Takeda, M. *et al. De novo* resistance to epidermal growth factor receptor–tyrosine kinase inhibitors in EGFR mutation-positive patients with non-small cell lung cancer. *J. Thorac. Oncol.* **5**, 399–400 (2010).
48. Egle, A., Harris, A.W., Bouillet, P. & Cory, S. Bim is a suppressor of Myc-induced mouse B cell leukemia. *Proc. Natl. Acad. Sci. USA* **101**, 6164–6169 (2004).

ONLINE METHODS

Ethics committee approval. Clinical CML samples were obtained from patients seen at the Singapore General Hospital, the Akita University Hospital, the University of Malaya Medical Centre and the National University Cancer Institute, Singapore. German control samples were obtained from blood donors at the University Hospital of Bonn. Malay, Chinese and Indian control samples were derived from recent local population studies[49,50]. Clinical NSCLC samples were obtained from patients seen at the National Cancer Centre, Singapore, the Toho University Omori Medical Center, Japan, the Aichi Cancer Center, Japan and the National University Cancer Institute, National University Health System, Singapore. Written informed consent and institutional review board approval at the participating institutions were obtained from all patients and normal individuals who contributed samples to this study.

DNA-PET sequencing and structural variation detection. DNA-PET sequencing and clustering of discordant PETs (dPETs) for structural variation detection has been described in Hillmer *et al.*[51]. DNA-PET libraries with 5-, 7- and 9-kb DNA fragments (**Supplementary Table 2**) were sequenced using the SOLiD platform (Applied Biosystems). The sequencing data from this study have been submitted to NCBI Gene Expression Omnibus (GEO) (http://www.ncbi.nlm.nih.gov/geo/) under accession number GSE28303 for the five patient samples and under accession number GSE26954 for K562. The genomic region that was covered by the 5′ tags of a dPET cluster was defined as the 5′ anchor, and the genomic region that was covered by the 3′ tags of a cluster was defined as the 3′ anchor. dPET clusters with anchor regions <500 bp were excluded from further analyses. The DNA-PET sequencing of K562 has been described earlier[51]. The same K562 dPET clusters used previously were also used in the present study, but the centromeric regions were not excluded here, dPET clusters with anchor regions <500 bp were excluded here (previously clusters with anchor regions <1,000 bp were excluded), and a new exclusion and filtering procedure was applied here (**Supplementary Note** and **Supplementary Table 13**).

Genotyping of the *BIM* polymorphic deletion. *Determination of patient genotype.* We extracted genomic DNA from either patients' peripheral blood (for both CML and NSCLC) or from formalin-fixed paraffin-embedded (FFPE) biopsy slides and blocks (for NSCLC). For DNA extracted from blood samples, we genotyped the deletion in the samples by a single PCR reaction using the primers 5′-AATACCACAGAGGCCCACAG-3′ and 5′-GCCTGAAGGTGCTGAGAAAG-3′ and JumpStart RedAccuTaq LA DNA Polymerase (Sigma) with the following thermo cycling conditions: 96 °C for 30 s, (94 °C for 15 s, 60 °C for 60 s and 68 °C for 10 min) ×29 and 68 °C for 20 min. The resulting PCR products from the deletion (1,323 bp) and the wild-type (4,226 bp) alleles were analyzed on 1% agarose gels.

For DNA recovered from FFPE tissues, we performed two separate PCR reactions to determine the presence of the wild-type and deletion alleles. The wild-type allele was genotyped using the forward primer 5′-CCA CCAATGGAAAAGGTTCA-3′ and the reverse primer 5′-CTGTCATTTC TCCCCACCAC-3′. The deletion allele was genotyped using the forward primer 5′-CCACCAATGGAAAAGGTTCA-3′ and the reverse primer 5′-GGC ACAGCCTCTATGGAGAA-3′. We performed PCR reactions using GoTaq Hot start Polymerase (Promega) with the following thermo cycling conditions: 95 °C for 5 min, (95 °C for 50 s, 58 °C for 50 s and 72 °C for 1 min) ×39 and 72 °C for 10 min. The PCR products for the deletion (284 bp) and the wild-type (362 bp) alleles were analyzed on a 2% agarose gel and were sequenced.

Determination of population frequency. We used Affymetrix Genome-Wide Human SNP Array 6.0 intensity data downloaded from the HapMap[52] homepage (http://snp.cshl.org/) to infer the copy number of the deletion polymorphism in *BIM* for the HapMap samples. Two genotyped single nucleotide positions were located within the deletion: SNP_A-4195083 and CN_173550. The raw intensities of the two markers were used to call the copy number variation event using a Gaussian mixture model similar to the algorithm proposed by Korn and colleagues[53]. Using this procedure, we predicted the copy number and, therefore, the presence or absence of the deletion in unrelated HapMap samples of European (n = 60), Yoruban (n = 60) and Chinese or Japanese (n = 90) origin. We then genotyped the deletion in the Chinese and Japanese samples for which we had available DNA (n = 74) by PCR as described above with the following slight modifications of the thermo cycling conditions: 96 °C for 30 s, (94 °C for 15 s, 64 °C for 30 s and 68 °C for 5 min) ×12, (94 °C for 15 s, 60 °C for 30 s and 68 °C for 5 min) ×18 and 68 °C for 20 min. We used the PCR-based genotypes to refine the single-nucleotide intensity cutoffs for genotype calling in the European and Yoruban samples and used only the PCR-validated genotypes of the East Asian samples for frequency assessment.

To investigate further whether the deletion in the European population is at moderate frequency but has been missed by chance in the HapMap samples and to determine more precisely the deletion frequency in Asia, we genotyped by PCR assay 595 German, 600 Malay, 608 Chinese and 605 Indian samples.

Calculation of attributable fractions for the *BIM* deletion. To calculate the population attributable fraction (PAF) of treatment resistance in East Asian patients, we used PAF = (f(OR − 1))/(f(OR − 1) + 1), where f is the frequency of deletion carriers among patients (f = 0.133), and OR is the odds ratio of the deletion carriers between patients being resistant and patients being sensitive to TKI treatment (OR = 2.94).

FISH. We used Vysis LSI (Locus specific identifier) BCR/ABL1 dual-fusion translocation probes (Abbott Molecular) for detecting *BCR-ABL1*. The LSI BCR probe is labeled with SpectrumGreen, and the LSI ABL1 probe is labeled with SpectrumOrange. We treated cells with 0.75 M KCl for 15 min at 37 °C. After fixation, we dropped the nuclei on slides for FISH according to the manufacturer's instructions with slight modifications. Briefly, we dehydrated the slides in a co-denaturated alcohol series for 3 min at 75 °C, which was followed by an overnight hybridization at 37 °C. We evaluated FISH signals in 200 interphase nuclei using a fluorescence microscope (Olympus BX60) under 1,000× magnification.

Cell lines, culture and chemicals. We purchased CML lines from American Type Culture Collection (ATCC) (MEG-01 and KU812), the Japanese Collection of Research Bioresources (NCO2) and the German Collection of Microorganisms and Cell Cultures (KCL22, K562, KYO-1, JK1, BV173 and NALM1). NSCLC cells (PC9 and HCC2279) were a gift from P. Koeffler. We cultured cells in RPMI-1640 medium supplemented with penicillin/streptomycin, glutamine and 10% FBS and incubated them in a humidified incubator at 37 °C with 5% CO_2. Zinc-finger-nuclease–edited K562 and PC9 cells were generated and maintained in RPMI-1640 medium supplemented with penicillin/streptomycin, glutamine and 20% FBS. Drugs were dissolved in DMSO (50% for imatinib; 100% for gefitinib and ABT-737) and kept at −20 °C. We used 1 μM imatinib and 0.5 μM gefitinib for all experiments, unless otherwise indicated. The treatment time was 12 h (**Figs. 2g** and **3d**), 24 h (**Figs. 2h–j** and **4**) or 48 h (**Fig. 3e–i**).

Real-time PCR analysis of exon-specific *BIM* transcripts. We extracted total cellular RNAs using the RNeasy Mini Kit (Qiagen). RNA was reverse transcribed using Superscript III First-Strand Synthesis System (Invitrogen) and quantitatively assessed using the iQ5 Multicolor Real-Time Detection System (Bio-Rad) with a total reaction volume of 25 μl. Primers were annealed at 59 °C for 20 s, and the amplicon was extended at 72 °C for 30 s. The total number of cycles quantified was 40. Transcript levels of β-actin or exon 2A of *BIM* were used to normalize between samples. The following primers were used: *BIM* exon 2A (forward: 5′-ATGGCAAAGCAACCTTCTGATG-3′; reverse: 5′-GGCTCTGTCTGTAGGGAGGT-3′), *BIM* exon 3 (forward: 5′-CA ATGGTAGTCATCCTAGAGG-3′; reverse: 5′-GACAAAATGCTCAAGGA AGAGG-3′), *BIM* exon 4 (forward: 5′-TTCCATGAGGCAGGCTGAAC-3′; reverse: 5′-CCTCCTTGCATAGTAAGCGTT-3′) and β-actin (forward: 5′-GGAC TTCGAGCAAGAGATGG-3′; reverse: 5′-AGCACTGTGTTGGCGTACAG-3′).

RT-PCR and sequencing of *BIM* transcripts. To assess whether the splicing of *BIM* exons 3 and 4 are indeed mutually exclusive, we performed RT-PCR and sequenced all *BIM* transcripts that were amplified. Total cellular RNA extraction and reverse transcription was performed using the method described above. We used the forward primer 5′-ATGGCAAAGCAACCTTCTGA-3′ and the reverse primer 5′-TCAATGCATTCTCCACACCA-3′ to amplify all transcripts that contained exons 2 and 5. These primers were annealed at 57 °C for 30 s, and the amplicons were extended at 72 °C for 1 min. To amplify transcripts containing

exon 3, we used the forward primer 5′-TGACTCTCGGACTGAGAAACG-3′ and the reverse primer 5′-CCAAAGCACAGTGAAAGATCA-3′. These primers were annealed at 55 °C for 30 s, and the amplicons were extended at 72 °C for 30 s. All PCR products were cloned into pJET1.2/blunt vector (Fermentas) before they were sent for sequencing analysis.

Western blot. We used antibodies to the following to perform western blotting: BCR-ABL1 (#2802), pBCR-ABL1 (#2861), BIM (#2819), CRKL (#3182), pCRKL (#3181), CASPASE 3 (#9662), cleaved CASPASE 3 (#9661), STAT5A (#9310), pSTAT5A (#9359), ribosomal protein S6 (RPS6; #2317), pRPS6 (#2211), PARP (#9542), phospho-EGFR (Y1068,#2234) (all from Cell Signaling Technology), Flag-M2 clone and β-actin (#AC-15, Sigma). The antibody dilutions used were 1 in 1,000, except for pRPS6 (1 in 2,000) and β-actin (1 in 5,000). A BIM-γ–specific antibody was generated by a commercial entity (Open Biosystems). HRP-conjugated secondary antibodies were specific to rabbit (Sigma) or mouse IgG (Santa Cruz biotechnology). The protein bands on the membrane were visualized using the Western Lightning chemiluminescence reagent (PerkinElmer).

Minigene vector construction. We used the pI-12 splicing vector (a gift from M. Garcia-Blanco) to construct the minigene vectors pI-12-MUT and pI-12-WT, which contained and did not contain the deletion polymorphism, respectively. Briefly, *BIM* exon 4, together with a 659-bp sequence upstream of exon 4, was amplified from KCL22 genomic DNA using forward primer 5′-GCC GCTCGAGTCTCTCCATGTGGTGTTTG-3′ and reverse primer 5′-GCC GAAGCTTCCTCCTTGCATAGTAAGCGTT-3′. The PCR product was subcloned into the XhoI and HindIII sites in the pI-12 plasmid to generate an intermediate vector. *BIM* exon 3 and the upstream region with and without the deletion polymorphism were amplified from KCL22 genomic DNA using forward primer 5′-GCCGGATATCATGGAAGGAACTGACCTGGTG-3′ and reverse primer 5′-GCCGATCGATGTAGGAAACTGGGTGAATGGC-3′. The two PCR products (4,500 bp and 1,597 bp) were subcloned into the *Eco*RV and *Cla*I sites in the intermediate vector to obtain the pI-12-WT and pI-12-MUT constructs. The ratios of exon 3 to exon 4 transcripts in the transfected cells were obtained by qPCR using specific primers for the U-E3 and U-E4 transcripts. Transcript levels were normalized to the adenovirus exonic sequence (U). The following primers were used: adenovirus exon (forward: 5′-CGA GCTCACTCTCTTCCGC-3′; reverse: 5′-CTGGTAGGGTACCTCGCA-3′), U-E3 transcript (forward: 5′- CGAGCTCACTCTCTTCCGC-3′; reverse: 5′-CTCTA GGATGACTACTGGTAGGGT-3′) and U-E4 transcript (forward: 5′-CGAGC TCACTCTCTTCCGC-3′; reverse: 5′- CCTCATGGAAGCTGGTAGGGT-3′).

siRNA knockdown of E3-containing *BIM* transcripts. siRNAs against E3-containing *BIM* transcripts (BIM-γ siRNA1: 5′-CCACCAUAGUCAAGAUACA-3′; BIM-γ siRNA2: 5′-CAGAACAACUCAACCACAA-3′) and negative control siRNA (ON-TARGETplus Non-targeting siRNA #1) were purchased from Dharmacon Inc (Lafayette). Nucleofection was performed on KCL22 cells using Nucleofector Solution V (Lonza) in the presence of siRNAs.

Determination of protein stability and apoptotic activity of different BIM isoforms. We cloned the complementary DNA of different BIM isoforms (BIMEL, BIML, BIMS and BIM-γ; gifts from A. Vazquez) into the pcDNA3-FLAG3 vector (a gift from K. Itahana). We transfected 5 μg of plasmid into KCL22 (**Supplementary Fig. 2e**) or K562 cells (**Supplementary Fig. 3a,b,d**) by nucleofection. To determine apoptotic activity, we used Annexin V-FITC and 7-AAD staining and flow cytometry. To determine the stability of the BIM-γ and BIML proteins, we treated transfected cells with 50 μg/ml of cycloheximide 44 h after nucleofection. Then we harvested the cells at various time points after treatment (0, 0.5, 1, 3, 5 and 7 h), and we determined the stability of Flag-tagged BIM-γ or BIML by western blot using antibodies to the Flag epitope.

Creation of *BIM* deletion polymorphism by ZFNs. The ZFN was custom made by Sigma-Aldrich CompoZr TM ZFN Technology with the following binding and cleavage sites: 5′-**CCTTCCCTGGAA**-ctggga-**ATAGTGGGTGAGATAGTG**-3′ (with the binding site in bold and the cleavage site not bolded). The cleavage site is located 551 bp downstream of the 5′ end of the *BIM* deletion polymorphism region. The repair template contained only the two flanking homology arms but not the *BIM* deletion polymorphism region. The repair template was constructed using a PCR strategy that used the KCL22 genomic DNA as a template and the forward primer 5′-CATAAATACCACAGAGGCCCACAGC-3′ (corresponding to a site 619 bp upstream from the 5′ end of the *BIM* deletion polymorphism) and reverse primer 5′-CCCTCGAAGACACCTCTATTGGGAGGC-3′ (corresponding to a site 743 bp downstream of the 3′ end of the *BIM* deletion polymorphism). We subcloned the 1,362-bp PCR product into the vector pCR-Blunt II-TOPO (Invitrogen), and we confirmed the correct template by sequencing.

The repair template and ZFN-encoding plasmids were transfected into K562 cells using the protocol mentioned previously[54]. To generate genome-edited cells, PC9 cells were seeded at a density of 2×10^5 cells per well in a six-well plate 1 d before transfection. The cells were transfected with the repair template (6 μg) and ZFN-encoding plasmids (0.6 μg each) using Fugene HD (Promega, USA). One day later, the transfected PC9 cells were arrested at the G2 phase for 18 h with 0.2 μM vinblastine (Sigma, USA). The cells were released from G2 arrest by washing twice in PBS, re-plating in a new tissue culture plate and being allowed to recover for 72 h.

We isolated the genome-edited K562 and PC9 clones by dilution cloning. We diluted the transfected cells to a density of 2.5 cells/ml and seeded 200 μl of the diluted cells into each well of a 96-well plate. Clones that successfully amplified from each well were harvested, and the genomic DNA was isolated using a Qiagen DNEasy kit (Hilden).

We screened for clones having the *BIM* deletion polymorphism by PCR using primers annealing to the *BIM* intronic region outside of the repair template, an approach that ensured the repair template would not be amplified. We used the forward primer 5′- GGCCTTCAACCACTATCTCAGTGCAATGG-3′ (corresponding to a site 1,507 bp upstream from the 5′ end of the *BIM* deletion polymorphism) and the reverse primer 5′-GGTTTCAGAGACAGAGCTGGG ACTCC-3′ (corresponding to a site 767 bp downstream of the 3′ end of the *BIM* deletion polymorphism) for PCR.

ELISA-based DNA fragmentation detection and western blotting on genome-edited K562 and PC9 clones. The presence of mono- and oligo-nucleosomes in the apoptotic cells was detected using the Cell Death Detection ELISA (Roche), following the manufacturer's instructions. Genome-edited K562 cells were seeded at a density of 2×10^5 cells/ml. Five milliliters or 0.5 ml of cells were used for western blot or the apoptotic assay, respectively. The cells were harvested 48 h after treatment. Genome-edited PC9 cells were seeded at a density of 5×10^4 cells/ml. Ten milliliters or 0.5 ml of cells were used for western blot or the apoptotic assay, respectively. The cells were harvested 24 h after treatment.

Apoptosis assay in primary CML samples. We measured apoptosis in primary CML samples using the Annexin V-FITC kit (Beckman Coulter, IN) with propidium iodine, following the manufacturer's instructions. Statistical significance was determined using a one-tailed Wilcoxon rank sum test, as deletion-containing cells are expected to be more resistant than non–deletion-containing cells.

Trypan blue assay. PC9 and HCC2279 cells (5×10^5 and 1.6×10^5 cells, respectively) were seeded in triplicate and treated for 48 h. The cells were trypsinized, and the number of viable cells was determined by trypan blue exclusion.

Mutation analysis for EGFR. FFPE slides of lung tumors were deparaffined by washing the slides in xylene and absolute ethanol. Lung cancer regions from each slide were scraped and transferred into a 1.5-ml tube, and genomic DNA was extracted using a QIAamp FFPE Tissue kit (Qiagen). EGFR exons 18–21 were sequenced. Fifty nanograms of FFPE genomic DNA was amplified by PCR in a 20 μl reaction volume containing 10 μl of GoTaq hot start Taq colorless master mix (M5133, Promega) in the following PCR conditions: 95 °C for 5 min, DNA amplification for 35 cycles at 95 °C for 50 s, 58 °C for 50 s, 72 °C for 60 s and a final extension at 72 °C for 10 min. The PCR primers used were: exon 18 (forward: 5′-TGGCACTGCTTTCCAGCATGG-3′; reverse: 5′-CTCCCCACCAGACCATGAGAGG-3′), exon 19 (forward: 5′-ATC ACTGGGCAGCATGTGGCA-3′; reverse: 5′-CCTGAGGTTCAGAGCCAT GGAC-3′), exon 20 (forward: 5′-CATGCGAAGCCACACTGACGTG-3′; reverse: 5′-GCATGTGAGGATCCTGGCTC-3′) and exon 21 (forward: 5′-GA TCTGTCCCTCACAGCAGG-3′; reverse: 5′-GGTGTCAGGAAAATGCTGG

CTG-3′). PCR products were purified by Exonuclease I (M0293L, New England Biolabs) and Shrimp Alkaline Phosphatase (Promega) treatments. Purified PCR products were sequenced in the forward and reverse directions using the ABI PRISM BigDye Terminator Cycle Sequencing Ready Reaction kit (Version 3) on an ABI PRISM 3730 Genetic Analyzer (Applied Biosystems, Foster City, California). Chromatograms were analyzed by SeqScape V2.5 and manual review.

Statistical analysis for PFS of patients with EGFR NSCLC. The primary endpoint in this study was to examine the effect of the *BIM* deletion polymorphism on the PFS of patients with EGFR-NSCLC from East Asian countries who were treated with EGFR TKIs. We calculated the PFS from the initiation of EGFR TKI therapy until either tumor progression or death from any cause. Observations were censored if TKI therapy was stopped because of side effects or if treatment was ongoing at the time of the analysis. We calculated the *P* values of the Kaplan-Meier test comparing survival curves using the Wilcoxon test. We used the *t* test and Fisher's exact test to test for differences between clinical characteristics of the *BIM*-deleted and wild-type populations. Using Cox proportional hazard regression analyses, univariate and multivariate hazard ratios were generated for the following factors: age, gender, histology, smoking history, type of EGFR mutation by exon and specific mutation, stage, first- or second-line TKI therapy, race, country (Japan or Singapore), TKI (gefitinib or erlotinib) and ECOG status. The significance level for entering variables in a stepwise regression was 0.05. We used the SAS System for Windows Version 9.2 LIFETEST, TTEST and PHREG procedures to perform the calculations.

49. Foong, A.W. *et al.* Rationale and methodology for a population-based study of eye diseases in Malay people: the Singapore Malay eye study (SiMES). *Ophthalmic Epidemiol.* **14**, 25–35 (2007).
50. Lavanya, R. *et al.* Methodology of the Singapore Indian Chinese Cohort (SICC) eye study: quantifying ethnic variations in the epidemiology of eye diseases in Asians. *Ophthalmic Epidemiol.* **16**, 325–336 (2009).
51. Hillmer, A.M. *et al.* Comprehensive long-span paired-end-tag mapping reveals characteristic patterns of structural variations in epithelial cancer genomes. *Genome Res.* **21**, 665–675 (2011).
52. Frazer, K.A. *et al.* A second generation human haplotype map of over 3.1 million SNPs. *Nature* **449**, 851–861 (2007).
53. Korn, J.M. *et al.* Integrated genotype calling and association analysis of SNPs, common copy number polymorphisms and rare CNVs. *Nat. Genet.* **40**, 1253–1260 (2008).
54. Urnov, F.D. *et al.* Highly efficient endogenous human gene correction using designed zinc-finger nucleases. *Nature* **435**, 646–651 (2005).

Published OnlineFirst May 21, 2012; DOI:10.1158/2159-8290.CD-12-0009

REVIEW

ALKoma: A Cancer Subtype with a Shared Target

Hiroyuki Mano

ABSTRACT Anaplastic lymphoma kinase (ALK) is a receptor-type protein tyrosine kinase that is currently the focus of much attention in oncology. ALK is rendered oncogenic as a result of its fusion to NPM1 in anaplastic large cell lymphoma, to TPM3 or TPM4 in inflammatory myofibroblastic tumor, to EML4 in non–small cell lung carcinoma, and to VCL in renal medullary carcinoma. It is also activated as a result of missense mutations in neuroblastoma and anaplastic thyroid cancer. Whereas these various tumors arise in different organs, they share activated ALK, and a marked clinical efficacy with ALK inhibitors has already been shown for some of the tumors with ALK fusions. One of such compound, crizotinib, is now approved in the United States for the treatment of lung cancer positive for *ALK* rearrangement. I propose that tumors carrying abnormal ALK as an essential growth driver be collectively termed "ALKoma."

Significance: ALK acquires transforming ability through gene fusion or missense mutation in a wide range of human cancers. Some of these cancers, which I propose be collectively referred to as "ALKoma," may all be effectively treated with small compounds or antibodies targeted to activated ALKs. *Cancer Discov; 2(6); 495–502. ©2012 AACR.*

INTRODUCTION

Anaplastic lymphoma kinase (ALK) is a protein tyrosine kinase (PTK) that possesses a single transmembrane domain and consists of 1,620 amino acid residues in humans (Fig. 1; refs. 1, 2). The extracellular region of ALK contains 2 MAM (meprin, A5 protein, and protein phosphatase μ) domains (3) and a putative ligand-binding domain. ALK is relatively isolated in the phylogenetic tree of the PTK superfamily, with its kinase domain sharing the highest sequence identity with that of the leukocyte receptor tyrosine kinase (LTK; 79% identity) and that of the proto-oncoprotein ROS1 (50% identity).

In the mouse, expression of ALK is prominent in the brain and peripheral nervous system of developing embryos, but it decreases rapidly after birth. In the adult human, ALK is expressed at a low level in the central nervous system but is not detected in other tissues (4). Given these expression profiles, ALK has been thought to play an important role in the development or orchestration of the nervous system. Surprisingly, however, homozygous deletion of *Alk* in mice does not give rise to any apparent anomalies in morphology, internal organs, or fertility, suggesting that the gene is not essential for mouse development (5). A more detailed analysis of *Alk* knockout mice revealed an increase in the number of hippocampal progenitor cells in the brain and an enhanced performance in a test of novel object recognition. Another strain of such mice manifested increased ethanol consumption compared with heterozygous controls (6). These observations thus suggest that ALK may contribute to behavioral control in adult mice.

The structure of ALK, together with its expression pattern, suggests that it may function as a cell surface receptor for specific ligands that may regulate the proliferation or differentiation of neural cells. In the fruit fly, jelly belly (jeb) binds and activates an ortholog of ALK (7), but a mammalian ortholog of jeb has not been identified. The growth factors pleiotrophin and midkine have been proposed as candidate ligands for mammalian ALK (8, 9), but this notion remains controversial (10), leaving the biologic relevance of pleiotrophin and midkine unclear.

ALK first emerged in the field of oncology in 1994 as a result of the identification of its fusion to nucleophosmin (NPM1) in anaplastic large cell lymphoma (ALCL; Figs. 1 and 2; refs. 11, 12). The NPM1 portion mediates constitutive dimerization and consequent activation of the NPM1-ALK fusion protein (13). In addition to NPM1-ALK, various other ALK fusion proteins have now been identified in ALCL, including TFG-ALK, ATIC-ALK, and CLTC-ALK. The next disease linked to ALK was inflammatory myofibroblastic

Author's Affiliations: Division of Functional Genomics, Jichi Medical University, Tochigi; Department of Medical Genomics, Graduate School of Medicine, University of Tokyo, Tokyo, Japan; and CREST, Japan Science and Technology Agency, Saitama, Japan

Corresponding Author: Hiroyuki Mano, Division of Functional Genomics, Jichi Medical University, 3311-1 Yakushiji, Shimotsukeshi, Tochigi 329-0498, Japan. Phone: 81-285-58-7449; Fax: 81-285-44-7322; E-mail: hmano@jichi.ac.jp

doi: 10.1158/2159-8290.CD-12-0009

Published OnlineFirst May 21, 2012; DOI:10.1158/2159-8290.CD-12-0009

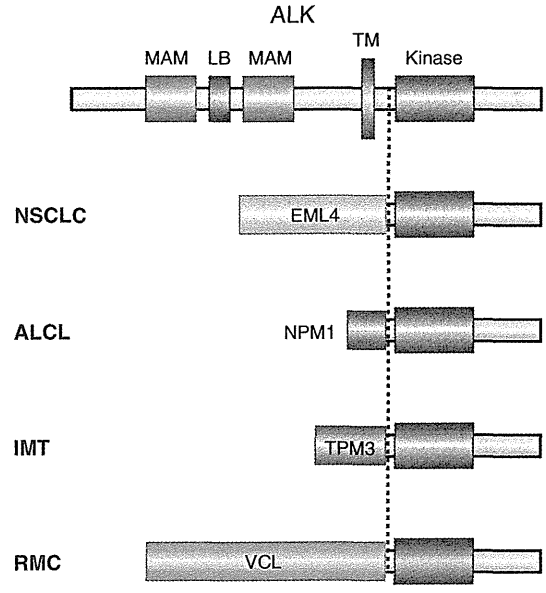

Figure 1. Structural organization of ALK and its fusion proteins. ALK is a receptor-type PTK with a single transmembrane (TM) domain as well as 2 MAM domains and a putative ligand-binding (LB) domain in the extracellular region. The intracellular region contains a kinase domain and is fused to EML4 in NSCLCs, to NPM1 in ALCLs, to TPM3 in IMTs, and to VCL in RMCs.

tumor (IMT), with increased expression of ALK and a rearranged *ALK* locus (chromosome band 2p23) being detected in a subset of IMT cases. A more detailed analysis identified *TPM3-ALK* and *TPM4-ALK* as fusion genes in IMT (Figs. 1 and 2; ref. 14). Further screening of IMT specimens revealed additional *ALK* fusions including *RANBP2-ALK* and *CARS-ALK*. Interestingly, some of these fusion genes, such as *TPM3/4-ALK* and *CLTC-ALK*, have been identified in both ALCLs and IMTs. The presence of *TPM3/4-ALK* was also reported in esophageal squamous cell carcinoma (15) and renal cancer (16).

In 2007, interest in ALK and the therapeutic potential of its specific inhibitors was boosted in response to the discovery of another fusion gene, *EML4-ALK*, this time in non-small cell lung carcinoma (NSCLC; ref. 17). Such interest was further increased the next year by the identification of activating point mutations in *ALK* in cases of neuroblastoma (18–21). In this review, I focus on activating genetic changes of *ALK* relevant to human cancer. Other aspects of *ALK* alterations (such as overexpression) in cancer have been elegantly reviewed elsewhere (22, 23).

EML4-ALK

EML4-ALK in NSCLC

Chronic myeloid leukemia (CML) is characterized by the presence of a fusion-type PTK, BCR-ABL1, that is generated as a result of a balanced chromosomal translocation, *t*(9;22). The remarkable therapeutic efficacy of the ABL1 inhibitor imatinib in individuals with this condition (24) suggested that targeting of the essential growth drivers in different types of cancer is a promising treatment strategy. To identify such growth drivers in clinical specimens, we developed a sensitive functional screening system based on retroviral cDNA expression libraries. The application of this approach to a lung adenocarcinoma specimen resulted in the discovery of *EML4-ALK* as a fusion-type oncogene (Figs. 1 and 2; ref. 17).

EML4 and *ALK* loci both map to the short arm of human chromosome 2 in opposite orientations and are separated by a distance of approximately 12 Mbp. A small inversion, inv(2)(p21p23), affecting both loci gives rise to the fusion gene. *EML4-ALK* was the first recurrent fusion-type oncogene in NSCLC, and, together with *ETS* fusions in prostate cancer (25), its existence argues against the previous notion that oncogenesis mediated by chromosome rearrangement is relatively specific to hematologic malignancies and sarcomas (rather than epithelial tumors).

EML4-ALK encodes a protein consisting of an amino-terminal portion of EML4 fused to the intracellular portion of ALK. EML4-ALK undergoes constitutive dimerization mediated through the coiled-coil domain of the EML4 portion and thereby acquires transforming ability in a manner

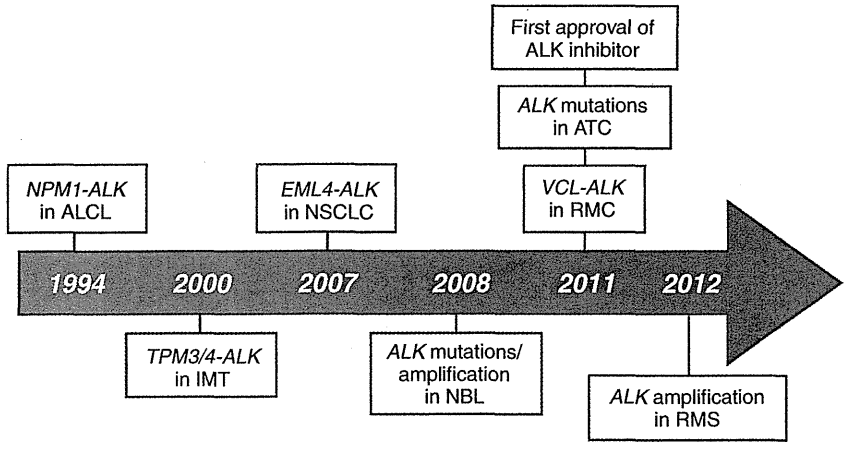

Figure 2. History of ALK in oncology. The first discovery of an oncogenic mutant of *ALK* was that of *NPM1-ALK* associated with ALCLs in 1994, which was followed by the identification of *TPM3/4-ALK* associated with IMTs, *EML4-ALK* associated with NSCLCs, mutated/amplified *ALK* associated with neuroblastoma (NBL), *VCL-ALK* associated with RMCs, mutated *ALK* associated with ATCs, and amplified *ALK* associated with rhabdomyosarcoma (RMS). Whereas several ALK inhibitors are currently in clinical trials, one such compound, crizotinib, was approved as a therapeutic drug for *ALK*-rearranged NSCLCs in 2011.

Published OnlineFirst May 21, 2012; DOI:10.1158/2159-8290.CD-12-0009

dependent on the associated upregulation of PTK activity. Indeed, several cell lines positive for *EML4-ALK* were found to be dependent on ALK catalytic activity for their proliferation (26, 27). Furthermore, transgenic mice that express *EML4-ALK* in lung type II alveolar cells manifest hundreds of adenocarcinoma nodules in both lungs soon after birth, and treatment of the animals with an ALK inhibitor results in the rapid clearance of these nodules (28). Such successful treatment of *EML4-ALK* transgenic mice with an ALK inhibitor was subsequently confirmed independently (29). These data suggested that EML4-ALK is the essential growth driver for NSCLC positive for this fusion kinase, and that targeting of ALK activity may therefore prove therapeutically effective in the clinic.

Clinicopathologic Features and Diagnosis of *EML4-ALK*–Positive Tumors

EML4-ALK is present in 3% to 6% of NSCLC cases (30–32). Of note, the clinical characteristics of patients with NSCLCs positive for *EML-ALK* are similar to those of such individuals who harbor activating mutations in the EGF receptor gene (*EGFR*): Both groups of patients thus tend to manifest an adenocarcinoma histology and to be non- or light smokers. However, the presence of *EML4-ALK* and that of *EGFR* or *KRAS* mutations are mutually exclusive, albeit with rare exceptions (33). Furthermore, whereas NSCLC with *EGFR* mutations is more prevalent in Asian populations than in Caucasians, no such ethnic differences have been reported for NSCLCs with *EML4-ALK*. With regard to pathologic characteristics, EML4-ALK–positive NSCLC has been found to contain signet-ring cells or to manifest a mucinous cribriform pattern (34–36), but other pathologic subtypes of NSCLCs also may harbor EML4-ALK. *EML4-ALK* may be infrequently present in other types of human cancers (16, 37).

The original *EML4-ALK* we identified resulted from ligation of intron 13 of *EML4* to intron 19 of *ALK* (17), but many other variants of the fusion gene have since been described. The vast majority of *ALK* translocations, including *EML4-ALK*, *NPM1-ALK*, and *TPM3-ALK*, involve intron 19 of *ALK*. Theoretically, ligation of *EML4* introns 1, 2, 6, 13, 18, 20, or 21 to intron 19 of *ALK* should generate an in-frame fusion at the mRNA level. Furthermore, given that exon 2 of *EML4* encodes the coiled-coil domain essential for EML4-ALK activation, all such fusions with the exception of that of *EML4* intron 1 would be expected to generate an oncogenic kinase. Large-scale screening of clinical specimens has revealed that the original *EML4-ALK* variant (referred to as E13;A20 or variant 1) together with a variant in which intron 6 of *EML4* is fused to intron 19 of *ALK* (referred to as E6;A20 or variant 3; ref. 26) account for more than 90% of all *EML4-ALK*–positive cases of NSCLCs in Japan (M. Soda, personal communication), but many rare variants have also been identified (17, 26, 27, 30, 31, 34, 37, 38).

Importantly, *EML4* exons theoretically unable to undergo in-frame fusion to exon 20 of *ALK* may be involved in the generation of oncogenic EML4-ALK proteins. For instance, an *EML4-ALK* cDNA in which exon 14 of *EML4* is fused in-frame to the 13th nucleotide of *ALK* exon 20 has been identified (30). In addition, another variant in which the nucleotide located 19 bp upstream of the 3′ end of *EML4* exon 15 is fused to that located 20 bp downstream of the 5′ end of *ALK* exon 20 was described (27). It is therefore important that clinics adopt diagnostic techniques, such as those based on multiplex reverse transcription PCR (RT-PCR), that are able to capture all these variants of *EML4-ALK* reliably.

Currently, no single technique may be suitable for the analysis of all specimen types. Immunohistochemistry and FISH, for example, are applicable to formalin-fixed, paraffin-embedded (FFPE) tissue specimens (32, 34, 35) but may not be suitable for the analysis of sputum, pleural effusion, bronchial lavage fluid, or frozen tissue. Conversely, the latter specimen types are readily examined by RT-PCR (30), whereas the former ones may not be suitable for this technique. I thus propose that diagnostic tools for the detection of EML4-ALK should be selected on the basis of the available specimen types. FISH and immunohistochemistry should be applied to FFPE tissue samples, whereas multiplex RT-PCR is appropriate for the other specimen types.

Crizotinib

The first ALK inhibitor to enter clinical trials was crizotinib, which is also known as PF-02341066 and is actually a dual inhibitor for both ALK and MET kinases (Table 1; ref. 39). At the time of the discovery of *EML4-ALK*, crizotinib had already entered a phase I trial that mainly targeted digestive tract cancers positive for *MET* amplification. After the report of *EML4-ALK*, the phase I trial with crizotinib was expanded to include tumors positive for ALK rearrangement, and the drug soon proved as therapeutically efficacious for such tumors.

Table 1. ALK inhibitors under clinical trials or already approved

Inhibitor	Company	Trial phase	References
Crizotinib	Pfizer	Phase III (approved in United States, South Korea, and Japan)	39, 68
CH5424802	Chugai Pharmaceutical	Phase I/II	62
ASP3026	Astellas Pharma	Phase I	Not available
LDK378	Novartis	Phase I	Not available
AP26113	Ariad	Phase I/II	61

Published OnlineFirst May 21, 2012; DOI:10.1158/2159-8290.CD-12-0009

The response rate for crizotinib in patients with *ALK*-rearranged NSCLCs in the trial was shown to be 57%, with a disease control rate of up to 90% (32). Furthermore, the median overall survival for crizotinib treatment was not determinable within the follow-up period of 18 months (40). Comparison of crizotinib treatment with a historical control was further striking. Whereas the median overall survival was not achieved for patients who received crizotinib as a second- or third-line treatment, it was only 6 months for the *ALK*-rearranged control patients who received conventional chemotherapy in the second- or third-line setting.

While crizotinib can inhibit MET kinase activity and *MET* may become amplified in NSCLCs (41), there was no *MET* amplification present in the above *EML4-ALK*–positive cohort (32). Similarly, while ROS1 tyrosine kinase is sensitive to crizotinib (42), a recent large-scale screening of gene fusions among NSCLC ($n = 1,529$) revealed a complete mutual exclusiveness between *ALK* and *ROS1* fusions (43). Furthermore, the mechanism for the insensitivity of *ALK* fusion–positive tumors to crizotinib has been mostly secondary mutations within the kinase domain of EML4-ALK (see below). These data evidence that crizotinib exerts its marked therapeutic efficacy in NSCLCs through specific suppression of EML4-ALK activity.

These observations clearly supported the clinical use of ALK inhibitors for the treatment of *EML4-ALK*–positive NSCLC. Indeed, on August 26, 2011, the U.S. Food and Drug Administration approved crizotinib as a treatment for *ALK*-rearranged NSCLCs. From the time of our first report of the identification of *EML4-ALK* in 2007, it took only 4 years for the first ALK inhibitor to be approved for use in the clinic, which is a record for cancer drug development (44).

OTHER *ALK* TRANSLOCATIONS IN EPITHELIAL TUMORS

Following the discovery of *EML4-ALK*, efforts have expanded to detect novel ALK fusions in epithelial tumors. Development of a sensitive immunohistochemical technique (intercalated antibody-enhanced polymer method, or iAEP) to stain ALK proteins in FFPE specimens led to the identification of several NSCLC samples that were positive with this approach but negative for *EML4-ALK* with multiplex RT-PCR (34). Further investigation of these specimens revealed the presence of another fusion of *ALK*, *KIF5B-ALK*. Similar to EML4-ALK, KIF5B contains dimerization motifs that play an essential role in the oncogenic activity of KIF5B-ALK and there are now known to be several variants of KIF5B-ALK (45). Togashi and colleagues reported still another *ALK* fusion, *KLC1-ALK*, in NSCLCs (46).

Yet another novel *ALK* fusion, *VCL-ALK*, was recently identified in a tumor of unclassified renal cell carcinoma with renal medullary carcinoma (RMC) characteristics that developed in a 16-year-old boy with sickle cell trait (47). VCL-ALK was also detected in RMCs isolated from a 6-year-old boy (48). RMC mostly affects young individuals and has a poor outcome, but the discovery of *VCL-ALK* has raised the possibility of effective treatment with an ALK inhibitor for patients who harbor this fusion gene. Furthermore, screening of tissue microarrays of renal cell carcinoma with the iAEP technique led to the detection of single cases each positive for *TPM3-ALK* or *EML4-ALK* (E2;A20 variant; ref. 16).

ONCOGENIC POINT MUTATIONS IN ALK

Neuroblastoma

Attempts by several groups to identify genes underlying neuroblastoma through different approaches (mapping of single-nucleotide polymorphisms for familial neuroblastoma and chromosome copy number analysis for sporadic neuroblastoma) resulted in the almost simultaneous identification of activating mutations within *ALK* (Figs. 2 and 3; refs. 18–21). About 10% of sporadic neuroblastoma cases harbor somatic nonsynonymous mutations within ALK, including K1062M, F1174L/C/I, F1245C/V/L, and R1275Q amino acid substitutions. On the other hand, a distinct but partially overlapping set of ALK mutations (T1087I, G1128A, R1275Q, and others) has been identified in familial neuroblastoma.

Importantly, these mutations do not confer equal transforming ability. The F1174L mutant, for instance, efficiently phosphorylates the signaling molecules STAT3 and AKT, but not extracellular signal–regulated kinase (ERK)1/2, whereas the R1275Q mutant efficiently phosphorylates ERK1/2 but not STAT3 (18). Knockdown experiments revealed that the growth of neuroblastoma cell lines was dependent to a greater extent on the F1174L mutant than on R1275Q (18, 20). The mutant ALK proteins thus contribute substantially to the transformation process in neuroblastoma, but the extent to which they do so varies among the mutation types.

These mutations also differentially affect the sensitivity of neuroblastoma to ALK inhibitors (49, 50), which may not be surprising given that point mutations within the kinase domain of ALK affect its 3-dimensional structure (including that of the inhibitor binding cleft) and thereby influence inhibitor binding. The F1174L mutant confers marked resistance to crizotinib in a cell-based assay (49, 50), suggesting that this amino acid substitution not only increases the enzymatic activity of ALK by changing the structure of the kinase domain but by doing so also affects the binding of ALK inhibitors.

The I1250T mutation of ALK was recently identified in an individual with neuroblastoma and was shown to abolish the activity of the enzyme (51). Each ALK mutation identified in neuroblastoma therefore needs to be assessed for how (or if) it contributes to carcinogenesis.

Anaplastic Thyroid Cancer

Nucleotide sequencing of *ALK* exons encoding the kinase domain in cell lines and fresh specimens of thyroid cancer (52) revealed novel missense mutations specifically in anaplastic thyroid cancer (ATC) samples (2 positive samples of 11). Each of the 2 identified amino acid substitutions (L1198F and G1201E) increased the enzymatic activity of ALK and induced the formation of transformed foci when introduced into mouse 3T3 cells, clearly indicating the activating nature of these mutations. It is thus likely that a subset of ATC and neuroblastoma cases share the same transforming gene, but it remains to be determined whether the *ALK* mutation profiles differ between the 2 disorders.

Published OnlineFirst May 21, 2012; DOI:10.1158/2159-8290.CD-12-0009

GENE AMPLIFICATION OF *ALK*

In addition to nonsynonymous mutations, *ALK* infrequently becomes amplified in neuroblastoma (21, 53). While its clinical relevance is yet to be clarified, *ALK* amplification frequently co-occurs with amplification of *MYCN* amplification, a known growth driver for this disorder, suggesting that *ALK* also contributes to carcinogenesis.

Recently, van Gaal and colleagues (54) have discovered frequent copy number gain of *ALK* in rhabdomyosarcoma accompanied with an increased level of ALK protein. In some cases, *ALK* copy number was even above 10. Interestingly, contrary to neuroblastoma, rhabdomyosarcoma with *ALK* amplification do not carry *MYCN* amplification. Such *ALK* anomaly is likely to be connected to carcinogenesis because *ALK* gain was associated with poor survival and the occurrence of metastases. In addition, van Gaal and colleagues also identified one case with ALK (D1225N) and 7 with *ALK* frameshift mutations of 43 rhabdomyosarcoma specimens, although clinical relevance of such mutations is yet to be examined.

RESISTANCE TO ALK INHIBITORS

Some EML4-ALK–positive NSCLC tumors are insensitive to initial treatment with ALK inhibitors, whereas others acquire resistance to these drugs after initial successful treatment. Information on the molecular mechanisms underlying such resistance remains limited.

The first insight into such resistance mechanisms was provided by analysis of an individual with EML4-ALK–positive NSCLC who initially showed a partial response to crizotinib treatment but underwent a rapid relapse after 5 months. *EML4-ALK* cDNA was amplified by PCR from tumor specimens obtained before the onset of treatment and after relapse, and it was then subjected to deep sequencing with a next-generation sequencer. Comparison of the 2 data sets resulted in the identification of 2 nonsynonymous mutations present only in the latter specimen. Interestingly, these 2 amino acid substitutions (C1156Y and L1196M) were found to independently confer resistance to crizotinib and other ALK inhibitors (55).

Neither C1156Y nor L1196M affects the enzymatic activity of EML4-ALK. NSCLC cells harboring either mutant might therefore be positively selected *in vivo* only in the presence of ALK inhibitors. Furthermore, Leu^{1196} is the "gatekeeper" site buried deeply within the ATP-binding pocket of ALK, with the corresponding sites of EGFR (Thr^{790}) and BCR-ABL1 (Thr^{315}) being the most frequently mutated residues associated with gefitinib and imatinib resistance, respectively (56).

Examination of a similar *EML4-ALK*–positive individual who initially responded to crizotinib but later acquired resistance revealed the presence in post-relapse *EML4-ALK* cDNA of a mutation resulting in an L1152R substitution in the kinase domain (57). Another mutation conferring drug resistance (F1174L) was identified in a case of RANBP2-ALK–positive IMTs (58). Of note, F1174L is also one of the frequent amino acid substitutions identified in neuroblastoma (Fig. 3). Further extensive screening of crizotinib-resistant mutations among 18 relapsed patients revealed 4 secondary mutations (1151Tins, L1196M, G1202R, and S1206Y) within the kinase domain of EML4-ALK, all of which confer resistance to ALK inhibitors (59). Such investigation further identified a high-level amplification of *EML4-ALK* in one patient, suggesting another mechanism (gene amplification) of drug insensitivity.

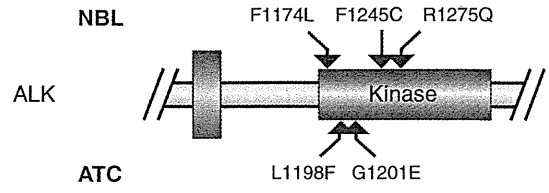

Figure 3. Missense mutations in ALKs. Activating mutations of ALKs are associated with familial and sporadic neuroblastoma (NBL). A different set of missense mutations is also associated with a subset of ATC tumors. Representative mutations for each disorder are shown according to their location in the kinase domain of ALK.

Another screening of *EML4-ALK*–positive tumors at a relapsed phase led to the identification of L1196M (in 2 of 14 resistant cases) and G1269A (in 2 cases) mutations accounting for the acquired drug resistance, and of gene amplification in 2 cases (60). Interestingly, in this cohort, some tumors lost *EML4-ALK* oncogene at the relapsed phase, but instead acquired activating *EGFR* or *KRAS* mutations. Whether such oncogenes other than *EML4-ALK* were present in a minor population of the original tumor or secondarily acquired during the crizotinib treatment remains elusive.

As of March 2012, 5 distinct ALK inhibitors are in clinical trials worldwide (Table 1), with some of these drugs showing inhibitory activity *in vitro* even with the gatekeeper mutant (61, 62). It will thus be of interest to determine whether treatment with such inhibitors results in the development of acquired resistance or not.

ALKOMA: A STEP TOWARD GENETIC INFORMATION–BASED CANCER CLASSIFICATION

Since the initial discovery of NPM1-ALK in 1994, our knowledge of the role of ALK in human cancer has increased markedly. We now recognize the contribution of ALK to an unexpectedly wide range of tumors, with *ALK* translocations underlying lymphoma, lung carcinoma, kidney cancer, and soft tissue tumors and *ALK* mutations being responsible for neuronal and thyroid cancer and *ALK* amplification frequently occurring in rhabdomyosarcoma.

Given that all ALK fusion kinases retain an intact ATP-binding pocket (where most ALK inhibitors bind), it is likely that ALK inhibitors will be effective against any tumor type that harbors such an ALK fusion (63, 64). From the standpoint of pharmaceutical companies, the fact that a single compound can serve as a magic pill for many different types of cancer in different organs is sufficiently compelling to warrant the development of such drugs even if the individual cancer types do not have a high incidence.

For neuroblastoma and ATC, however, the efficacy of an ALK inhibitor may be substantially influenced by the type or position of the missense mutation. However, given that ALK is a transmembrane protein, the mutant proteins may

Published OnlineFirst May 21, 2012; DOI:10.1158/2159-8290.CD-12-0009

be effectively targeted by antibodies (65), as is the case for other transmembrane proteins targeted by the antibodies rituximab and trastuzumab.

Genetic information was first integrated into the classification of hematologic malignancies. For instance, whereas acute myeloid leukemia (AML) had previously been divided into subgroups with distinct differentiation profiles (assessed by pathologic analyses), AML harboring *RUNX1-RUNX1T1*, *PML-RARA*, or *MLL* rearrangements is now defined as a distinct entity according to the current World Health Organization classification (66). Likewise, all-*trans* retinoic acid is highly effective only in the treatment of retinoic acid receptor alpha (encoded by *RARA*) fusion-positive AML, acute promyelocytic leukemia (APL). Similarly, ABL1 inhibitors are only used against *BCR-ABL1*–positive CML/acute lymphoblastic leukemia. It is likely that tumor cells of APL or CML are deeply addicted to the activity of PML-RARA or BCR-ABL1, respectively. Therefore, single reagents targeting individual oncoproteins have a profound therapeutic effect.

In the treatment of epithelial tumors, single EGFR inhibitors provide a high response rate to NSCLCs harboring activating *EGFR* mutations as well. Importantly, treatment with such EGFR inhibitors worsens the prognosis of NSCLC without *EGFR* mutations (67). Targeted drugs are, thus, likely to be highly effective only against tumors in which corresponding targets carry activating mutations and become "essential growth drivers" for the cancer. The definition of essential growth drivers for given oncogenes is difficult because treatment efficacy for cell lines *in vitro* does not always recapitulate that in clinics. For instance, while inhibitors against RAS or PIK3CA are able to suppress the growth of cancer cell lines, these compounds have failed to provide such efficacy in humans.

Therefore, significant response in patients by a monotherapy with a targeted drug should be a faithful indicator for the corresponding target to be the essential growth driver. Unfortunately, however, such clinically proven drivers are still few, but EML4-ALK is a newcomer to this growing list. Importantly, other ALK fusions, NPM1-ALK and RANBP2-ALK, are likely the essential growth drivers as well, because the crizotinib monotherapy has a profound therapeutic effect (63, 64). I propose that these tumors be collectively referred to as "ALKoma," in which abnormal ALK plays an indispensable component in the carcinogenesis.

Interestingly, the term "ALKoma" encompasses multiple organs. NSCLCs, IMTs, and ALCLs were once regarded as completely distinct clinical entities affecting different organs. However, it is now known that a fraction of each of these cancer types shares activated ALK as the essential growth driver and such tumors can be targeted for treatment with ALK inhibitors (32, 63, 64). Because of the similar protein structure to that of EML4-ALK/NPM1-ALK/RANBP2-ALK, VCL-ALK in RMCs should be a good candidate for the next member of ALKoma. Data from ongoing clinical trials with crizotinib for neuroblastoma will also tell us whether activated ALK with nonsynonymous mutations is also a strong driver for this disorder. The term "ALKoma" has the advantage that it indicates the preferred treatment for the tumor. It is thus a good example of genetic information–based "beyond organ" cancer classification, many other examples of which may emerge in the future.

Disclosure of Potential Conflicts of Interest

H. Mano has commercial research grant from Astellas Pharma and Illumina Inc.; Ownership Interest (including patents); and serves as a scientific advisor for Pfizer Inc., Astellas Pharma, Chugai Pharmaceutical, and Daiichi Sankyo Co., Ltd., and is an CEO of CureGene Co., Ltd.

Author's Contributions

Conception and design: H. Mano
Analysis and interpretation of data (e.g., statistical analysis, biostatistics, computational analysis): H. Mano
Writing, review, and/or revision of the manuscript: H. Mano
Study supervision: H. Mano

Acknowledgments

The author apologizes to all the authors whose work could not be included in the manuscript owing to space constraints and also thanks the members of his laboratory as well as K. Takeuchi for their dedication and support.

Grant Support

This work was supported in part by a grant for Research on Human Genome Tailor-made from the Ministry of Health, Labor, and Welfare of Japan as well as by a Grant-in-Aid for Scientific Research on Priority Areas from the Ministry of Education, Culture, Sports, Science, and Technology of Japan.

Received January 6, 2012; revised April 20, 2012; accepted April 20, 2012; published OnlineFirst May 21, 2012.

REFERENCES

1. Morris SW, Naeve C, Mathew P, James PL, Kirstein MN, Cui X, et al. ALK, the chromosome 2 gene locus altered by the t(2;5) in non-Hodgkin's lymphoma, encodes a novel neural receptor tyrosine kinase that is highly related to leukocyte tyrosine kinase (LTK). Oncogene 1997;14:2175–88.
2. Iwahara T, Fujimoto J, Wen D, Cupples R, Bucay N, Arakawa T, et al. Molecular characterization of ALK, a receptor tyrosine kinase expressed specifically in the nervous system. Oncogene 1997;14:439–49.
3. Beckmann G, Bork P. An adhesive domain detected in functionally diverse receptors. Trends Biochem Sci 1993;18:40–1.
4. Pulford K, Lamant L, Morris SW, Butler LH, Wood KM, Stroud D, et al. Detection of anaplastic lymphoma kinase (ALK) and nucleolar protein nucleophosmin (NPM)-ALK proteins in normal and neoplastic cells with the monoclonal antibody ALK1. Blood 1997;89:1394–404.
5. Bilsland JG, Wheeldon A, Mead A, Znamenskiy P, Almond S, Waters KA, et al. Behavioral and neurochemical alterations in mice deficient in anaplastic lymphoma kinase suggest therapeutic potential for psychiatric indications. Neuropsychopharmacology 2008;33:685–700.
6. Lasek AW, Lim J, Kliethermes CL, Berger KH, Joslyn G, Brush G, et al. An evolutionary conserved role for anaplastic lymphoma kinase in behavioral responses to ethanol. PLoS One 2011;6:e22636.
7. Lee HH, Norris A, Weiss JB, Frasch M. Jelly belly protein activates the receptor tyrosine kinase Alk to specify visceral muscle pioneers. Nature 2003;425:507–12.
8. Stoica GE, Kuo A, Aigner A, Sunitha I, Souttou B, Malerczyk C, et al. Identification of anaplastic lymphoma kinase as a receptor for the growth factor pleiotrophin. J Biol Chem 2001;276:16772–9.
9. Stoica GE, Kuo A, Powers C, Bowden ET, Sale EB, Riegel AT, et al. Midkine binds to anaplastic lymphoma kinase (ALK) and acts as a growth factor for different cell types. J Biol Chem 2002;277:35990–8.
10. Mathivet T, Mazot P, Vigny M. In contrast to agonist monoclonal antibodies, both C-terminal truncated form and full length form of Pleiotrophin failed to activate vertebrate ALK (anaplastic lymphoma kinase)? Cell Signal 2007;19:2434–43.

Published OnlineFirst May 21, 2012; DOI:10.1158/2159-8290.CD-12-0009

11. Morris SW, Kirstein MN, Valentine MB, Dittmer KG, Shapiro DN, Saltman DL, et al. Fusion of a kinase gene, ALK, to a nucleolar protein gene, NPM, in non-Hodgkin's lymphoma. Science 1994;263:1281–4.
12. Shiota M, Fujimoto J, Semba T, Satoh H, Yamamoto T, Mori S. Hyperphosphorylation of a novel 80 kDa protein-tyrosine kinase similar to Ltk in a human Ki-1 lymphoma cell line, AMS3. Oncogene 1994;9:1567–74.
13. Pulford K, Lamant L, Espinos E, Jiang Q, Xue L, Turturro F, et al. The emerging normal and disease-related roles of anaplastic lymphoma kinase. Cell Mol Life Sci 2004;61:2939–53.
14. Lawrence B, Perez-Atayde A, Hibbard MK, Rubin BP, Dal Cin P, Pinkus JL, et al. TPM3-ALK and TPM4-ALK oncogenes in inflammatory myofibroblastic tumors. Am J Pathol 2000;157:377–84.
15. Jazii FR, Najafi Z, Malekzadeh R, Conrads TP, Ziaee AA, Abnet C, et al. Identification of squamous cell carcinoma associated proteins by proteomics and loss of beta tropomyosin expression in esophageal cancer. World J Gastroenterol 2006;12:7104–12.
16. Sugawara E, Togashi Y, Kuroda N, Sakata S, Hatano S, Asaka R, et al. Identification of anaplastic lymphoma kinase fusions in renal cancer: large-scale immunohistochemical screening by the intercalated antibody-enhanced polymer method. Cancer. 2012 Jan 7. [Epub ahead of print]
17. Soda M, Choi YL, Enomoto M, Takada S, Yamashita Y, Ishikawa S, et al. Identification of the transforming *EML4-ALK* fusion gene in non-small-cell lung cancer. Nature 2007;448:561–6.
18. Mosse YP, Laudenslager M, Longo L, Cole KA, Wood A, Attiyeh EF, et al. Identification of ALK as a major familial neuroblastoma predisposition gene. Nature 2008;455:930–5.
19. Janoueix-Lerosey I, Lequin D, Brugieres L, Ribeiro A, de Pontual L, Combaret V, et al. Somatic and germline activating mutations of the ALK kinase receptor in neuroblastoma. Nature 2008;455:967–70.
20. George RE, Sanda T, Hanna M, Frohling S, Luther W II, Zhang J, et al. Activating mutations in ALK provide a therapeutic target in neuroblastoma. Nature 2008;455:975–8.
21. Chen Y, Takita J, Choi YL, Kato M, Ohira M, Sanada M, et al. Oncogenic mutations of ALK kinase in neuroblastoma. Nature 2008;455:971–4.
22. Barreca A, Lasorsa E, Riera L, Machiorlatti R, Piva R, Ponzoni M, et al. Anaplastic lymphoma kinase in human cancer. J Mol Endocrinol 2011;47:R11–23.
23. Pulford K, Morris SW, Turturro F. Anaplastic lymphoma kinase proteins in growth control and cancer. J Cell Physiol 2004;199:330–58.
24. Druker BJ, Talpaz M, Resta DJ, Peng B, Buchdunger E, Ford JM, et al. Efficacy and safety of a specific inhibitor of the BCR-ABL tyrosine kinase in chronic myeloid leukemia. N Engl J Med 2001;344:1031–7.
25. Tomlins SA, Rhodes DR, Perner S, Dhanasekaran SM, Mehra R, Sun XW, et al. Recurrent fusion of TMPRSS2 and ETS transcription factor genes in prostate cancer. Science 2005;310:644–8.
26. Choi YL, Takeuchi K, Soda M, Inamura K, Togashi Y, Hatano S, et al. Identification of novel isoforms of the *EML4-ALK* transforming gene in non-small cell lung cancer. Cancer Res 2008;68:4971–6.
27. Koivunen JP, Mermel C, Zejnullahu K, Murphy C, Lifshits E, Holmes AJ, et al. EML4-ALK fusion gene and efficacy of an ALK kinase inhibitor in lung cancer. Clin Cancer Res 2008;14:4275–83.
28. Soda M, Takada S, Takeuchi K, Choi YL, Enomoto M, Ueno T, et al. A mouse model for *EML4-ALK*-positive lung cancer. Proc Natl Acad Sci U S A 2008;105:19893–7.
29. Chen Z, Sasaki T, Tan X, Carretero J, Shimamura T, Li D, et al. Inhibition of ALK, PI3K/MEK, and HSP90 in murine lung adenocarcinoma induced by EML4-ALK fusion oncogene. Cancer Res 2010;70:9827–36.
30. Takeuchi K, Choi YL, Soda M, Inamura K, Togashi Y, Hatano S, et al. Multiplex reverse transcription-PCR screening for EML4-ALK fusion transcripts. Clin Cancer Res 2008;14:6618–24.
31. Wong DW, Leung EL, So KK, Tam IY, Sihoe AD, Cheng LC, et al. The EML4-ALK fusion gene is involved in various histologic types of lung cancers from nonsmokers with wild-type EGFR and KRAS. Cancer 2009;115:1723–33.
32. Kwak EL, Bang YJ, Camidge DR, Shaw AT, Solomon B, Maki RG, et al. Anaplastic lymphoma kinase inhibition in non-small-cell lung cancer. N Engl J Med 2010;363:1693–703.
33. Tiseo M, Gelsomino F, Boggiani D, Bortesi B, Bartolotti M, Bozzetti C, et al. EGFR and EML4-ALK gene mutations in NSCLC: a case report of erlotinib-resistant patient with both concomitant mutations. Lung Cancer 2011;71:241–3.
34. Takeuchi K, Choi YL, Togashi Y, Soda M, Hatano S, Inamura K, et al. KIF5B-ALK, a novel fusion oncokinase identified by an immunohistochemistry-based diagnostic system for ALK-positive lung cancer. Clin Cancer Res 2009;15:3143–9.
35. Mino-Kenudson M, Chirieac LR, Law K, Hornick JL, Lindeman N, Mark EJ, et al. A novel, highly sensitive antibody allows for the routine detection of ALK-rearranged lung adenocarcinomas by standard immunohistochemistry. Clin Cancer Res 2010;16:1561–71.
36. Yoshida A, Tsuta K, Nakamura H, Kohno T, Takahashi F, Asamura H, et al. Comprehensive histologic analysis of ALK-rearranged lung carcinomas. Am J Surg Pathol 2011;35:1226–34.
37. Lin E, Li L, Guan Y, Soriano R, Rivers CS, Mohan S, et al. Exon array profiling detects EML4-ALK fusion in breast, colorectal, and non-small cell lung cancers. Mol Cancer Res 2009;7:1466–76.
38. Sanders HR, Li HR, Bruey JM, Scheerle JA, Meloni-Ehrig AM, Kelly JC, et al. Exon scanning by reverse transcriptase-polymerase chain reaction for detection of known and novel EML4-ALK fusion variants in non-small cell lung cancer. Cancer Genet 2011;204:45–52.
39. Christensen JG, Zou HY, Arango ME, Li Q, Lee JH, McDonnell SR, et al. Cytoreductive antitumor activity of PF-2341066, a novel inhibitor of anaplastic lymphoma kinase and c-Met, in experimental models of anaplastic large-cell lymphoma. Mol Cancer Ther 2007;6:3314–22.
40. Shaw AT, Yeap BY, Solomon BJ, Riely GJ, Gainor J, Engelman JA, et al. Effect of crizotinib on overall survival in patients with advanced non-small-cell lung cancer harbouring ALK gene rearrangement: a retrospective analysis. Lancet Oncol 2011;12:1004–12.
41. Engelman JA, Zejnullahu K, Mitsudomi T, Song Y, Hyland C, Park JO, et al. MET amplification leads to gefitinib resistance in lung cancer by activating ERBB3 signaling. Science 2007;316:1039–43.
42. Bergethon K, Shaw AT, Ignatius Ou SH, Katayama R, Lovly CM, McDonald NT, et al. ROS1 rearrangements define a unique molecular class of lung cancers. J Clin Oncol 2012;30:863–70.
43. Takeuchi K, Soda M, Togashi Y, Suzuki R, Sakata S, Hatano S, et al. RET, ROS1 and ALK fusions in lung cancer. Nat Med 2012;18:378–81.
44. Gerber DE, Minna JD. ALK inhibition for non-small cell lung cancer: from discovery to therapy in record time. Cancer Cell 2010;18:548–51.
45. Wong DW, Leung EL, Wong SK, Tin VP, Sihoe AD, Cheng LC, et al. A novel KIF5B-ALK variant in nonsmall cell lung cancer. Cancer 2011;117:2709–18.
46. Togashi Y, Soda M, Sakata S, Sugawara E, Hatano S, Asaka R, et al. KLC1-ALK: a novel fusion in lung cancer identified using a formalin-fixed paraffin-embedded tissue only. PLoS One 2012;7:e31323.
47. Debelenko LV, Raimondi SC, Daw N, Shivakumar BR, Huang D, Nelson M, et al. Renal cell carcinoma with novel VCL-ALK fusion: new representative of ALK-associated tumor spectrum. Mod Pathol 2011;24:430–42.
48. Marino-Enriquez A, Ou WB, Weldon CB, Fletcher JA, Perez-Atayde AR. ALK rearrangement in sickle cell trait-associated renal medullary carcinoma. Genes Chromosomes Cancer 2011;50:146–53.
49. Bresler SC, Wood AC, Haglund EA, Courtright J, Belcastro LT, Plegaria JS, et al. Differential inhibitor sensitivity of anaplastic lymphoma kinase variants found in neuroblastoma. Sci Transl Med 2011;3:108ra14.
50. Schonherr C, Ruuth K, Yamazaki Y, Eriksson T, Christensen J, Palmer RH, et al. Activating ALK mutations found in neuroblastoma are inhibited by crizotinib and NVP-TAE684. Biochem J 2011;440:405–13.
51. Schonherr C, Ruuth K, Eriksson T, Yamazaki Y, Ottmann C, Combaret V, et al. The neuroblastoma ALK(I1250T) mutation is a kinase-dead RTK *in vitro* and *in vivo*. Transl Oncol 2011;4:258–65.
52. Murugan AK, Xing M. Anaplastic thyroid cancers harbor novel oncogenic mutations of the ALK gene. Cancer Res 2011;71:4403–11.
53. Bagci O, Tumer S, Olgun N, Altungoz O. Copy number status and mutation analyses of anaplastic lymphoma kinase (ALK) gene in 90 sporadic neuroblastoma tumors. Cancer Lett 2012;317:72–7.

Published OnlineFirst May 21, 2012; DOI:10.1158/2159-8290.CD-12-0009

54. van Gaal JC, Flucke UE, Roeffen MH, de Bont ES, Sleijfer S, Mavinkurve-Groothuis AM, et al. Anaplastic lymphoma kinase aberrations in rhabdomyosarcoma: clinical and prognostic implications. J Clin Oncol 2012;30:308–15.
55. Choi YL, Soda M, Yamashita Y, Ueno T, Takashima J, Nakajima T, et al. EML4-ALK mutations in lung cancer that confer resistance to ALK inhibitors. N Engl J Med 2010;363:1734–9.
56. Carter TA, Wodicka LM, Shah NP, Velasco AM, Fabian MA, Treiber DK, et al. Inhibition of drug-resistant mutants of ABL, KIT, and EGF receptor kinases. Proc Natl Acad Sci U S A 2005;102:11011–6.
57. Sasaki T, Koivunen J, Ogino A, Yanagita M, Nikiforow S, Zheng W, et al. A novel ALK secondary mutation and EGFR signaling cause resistance to ALK kinase inhibitors. Cancer Res 2011;71:6051–60.
58. Sasaki T, Okuda K, Zheng W, Butrynski J, Capelletti M, Wang L, et al. The neuroblastoma-associated F1174L ALK mutation causes resistance to an ALK kinase inhibitor in ALK-translocated cancers. Cancer Res 2010;70:10038–43.
59. Katayama R, Shaw AT, Khan TM, Mino-Kenudson M, Solomon BJ, Halmos B, et al. Mechanisms of acquired crizotinib resistance in ALK-rearranged lung cancers. Sci Transl Med 2012;4:120ra17.
60. Doebele RC, Pilling AB, Aisner DL, Kutateladze TG, Le AT, Weickhardt AJ, et al. Mechanisms of resistance to crizotinib in patients with ALK gene rearranged non-small cell lung cancer. Clin Cancer Res 2012;18:1472–82.
61. Katayama R, Khan TM, Benes C, Lifshits E, Ebi H, Rivera VM, et al. Therapeutic strategies to overcome crizotinib resistance in non-small cell lung cancers harboring the fusion oncogene EML4-ALK. Proc Natl Acad Sci U S A 2011;108:7535–40.
62. Sakamoto H, Tsukaguchi T, Hiroshima S, Kodama T, Kobayashi T, Fukami TA, et al. CH5424802, a selective ALK inhibitor capable of blocking the resistant gatekeeper mutant. Cancer Cell 2011;19:679–90.
63. Butrynski JE, D'Adamo DR, Hornick JL, Dal Cin P, Antonescu CR, Jhanwar SC, et al. Crizotinib in ALK-rearranged inflammatory myofibroblastic tumor. N Engl J Med 2010;363:1727–33.
64. Gambacorti-Passerini C, Messa C, Pogliani EM. Crizotinib in anaplastic large-cell lymphoma. N Engl J Med 2011;364:775–6.
65. Wellstein A, Toretsky JA. Hunting ALK to feed targeted cancer therapy. Nat Med 2011;17:290–1.
66. Vardiman JW, Thiele J, Arber DA, Brunning RD, Borowitz MJ, Porwit A, et al. The 2008 revision of the World Health Organization (WHO) classification of myeloid neoplasms and acute leukemia: rationale and important changes. Blood 2009;114:937–51.
67. Mok TS, Wu YL, Thongprasert S, Yang CH, Chu DT, Saijo N, et al. Gefitinib or carboplatin-paclitaxel in pulmonary adenocarcinoma. N Engl J Med 2009;361:947–57.
68. Zou HY, Li Q, Lee JH, Arango ME, McDonnell SR, Yamazaki S, et al. An orally available small-molecule inhibitor of c-Met, PF-2341066, exhibits cytoreductive antitumor efficacy through antiproliferative and antiangiogenic mechanisms. Cancer Res 2007;67:4408–17.

Lung Cancer 75 (2012) 66–72

Contents lists available at ScienceDirect

Lung Cancer

journal homepage: www.elsevier.com/locate/lungcan

ALK fusion gene positive lung cancer and 3 cases treated with an inhibitor for ALK kinase activity

Hideki Kimura[a,*], Takahiro Nakajima[a,d], Kengo Takeuchi[b], Manabu Soda[c], Hiroyuki Mano[c], Toshihiko Iizasa[a], Yukiko Matsui[a], Mitsuru Yoshino[a], Masato Shingyoji[a], Meiji Itakura[a], Makiko Itami[e], Dai Ikebe[e], Sana Yokoi[f], Hajime Kageyama[f], Miki Ohira[g], Akira Nakagawara[h]

[a] Division of Thoracic Diseases, Chiba Cancer Center, Chiba, Japan
[b] Pathology Project for Molecular Targets, Cancer Institute, Japanese Foundation for Cancer Research (JFCR), Koto, Tokyo, Japan
[c] Division of Functional Genomics, Jichi Medical University, Tochigi, Japan
[d] Division of Thoracic Surgery, Toronto General Hospital, University Health Network, Toronto, Canada
[e] Division of Pathology, Chiba Cancer Center, Japan
[f] Cancer Genome Center, Chiba Cancer Center Research Institute, Japan
[g] Laboratory of Cancer Genomics, Chiba Cancer Center Research Institute, Japan
[h] Chiba Cancer Center, Japan

ARTICLE INFO

Article history:
Received 16 October 2010
Received in revised form 24 May 2011
Accepted 30 May 2011

Key words:
ALK
EML4
KIF5B
Fusion gene
Lung cancer
EBUS
TBNA
Crizotinib
ALK inhibitor

ABSTRACT

Background: Anaplastic lymphoma kinase (ALK) fusion gene-positive lung cancer accounts for 4–5% of non-small cell lung carcinoma. A clinical trial of the specific inhibitor of ALK fusion-type tyrosine kinase is currently under way.
Methods: ALK fusion gene products were analyzed immunohistochemically with the materials obtained by surgery or by endobronchial ultrasound-guided transbronchial needle aspiration (EBUS-TBNA). The echinoderm microtubule-associated protein-like 4(EML4)-ALK or kinesin family member 5B (KIF5B)-ALK translocation was confirmed by the reverse transcription polymerase chain reaction (RT-PCR) and fluorescence in situ hybridization (FISH). After eligibility criteria were met and informed consent was obtained, 3 patients were enrolled for the Pfizer Study of Crizotinib (PF02341066), Clinical Trial A8081001, conducted at Seoul National University.
Results: Out of 404 cases, there were 14 of EML4-ALK non-small cell carcinoma (NSCLC) and one KIF5B-ALK NSCLC case (8 men, 7 women; mean age, 61.9 years, range 48–82). Except for 2 light smokers, all patients were non-smokers. All cases were of adenocarcinoma with papillary or acinar subtypes. Three were of stage IA, 5 of stage IIIA, 1 of stage IIIB and 6 of stage IV. Ten patients underwent thoracotomy, 3 received chemotherapy and 2 only best supportive care (BSC). One BSC and 2 chemotherapy cases were enrolled for the clinical trial. Patients with advanced stages who received chemotherapy or best supportive care were younger (54.0 ± 6.3) than those who were surgically treated (65.8 ± 10.1) ($p < 0.05$).
The powerful effect of ALK inhibitor on EML4-ALK NSCLC was observed. Soon after its administration, almost all the multiple bone and lymph node metastases quickly disappeared. Nausea, diarrhea and the persistence of a light image were the main side effects, but they diminished within a few months.
Conclusion: ALK-fusion gene was found in 3.7% (15/404) NSCLC cases and advanced disease with this fusion gene was correlated with younger generation. The ALK inhibitor presented in this study is effective in EML4-ALK NSCLC cases. A further study will be necessary to evaluate the clinical effectiveness of this drug.

1. Introduction

As the mechanisms of carcinogenesis become clearer, the target of cancer treatment is shifting from non-specific cytotoxic agents to specific agents that block key molecular events in the carcinogenesis of malignancy such as EGFR-TKI and anti-HER2 antibody (trastuzumab) [1–3]. Recently, Mano et al. [4–6] reported that a small inversion within chromosome 2p results in the formation of a fusion gene comprising portions of the

* Corresponding author at: Division of Thoracic Diseases, Chiba Cancer Center, 666-2, Nitona-cho, Chuo-ku, 260-8717 Chiba, Japan. Tel.: +81 43 264 5431; fax: +81 43 262 8680.
E-mail address: hkimura@chiba-cc.jp (H. Kimura).

0169-5002/$ – see front matter © 2011 Elsevier Ireland Ltd. All rights reserved.
doi:10.1016/j.lungcan.2011.05.027

echinoderm microtubule-associated protein-like 4 (EML4) gene and the anaplastic lymphoma kinase (ALK) gene in non-small-cell lung cancer. Transgenic mice that express EML4-ALK specifically in lung epithelial cells develop multiple foci of adenocarcinoma in the lung soon after birth, and the oral administration of a specific inhibitor of ALK tyrosine kinase activity eradicated completely the foci of adenocarcinoma. Clinical trials of specific inhibitors of EML4-ALK tumors are currently underway [7–11]. Kwak et al. [11] reported the effect of crizotinib in Clinical Trial A8081001 on the 82 patients with advanced ALK-positive disease. Over a mean treatment duration of 6.4 months, the overall response rate was 57% and the estimated probability of 6-month progression-free survival was 72%. We report 15 cases of ALK fusion gene-positive NSCLC cases and 3 cases in our experience with ALK inhibitor in the Pfizer Study of crizotinib (PF02341066), Clinical Trial A8081001, which was conducted at Seoul National University.

2. Materials and methods

Out of 404 patients who had undergone surgical resection (295 cases) or bronchoscopy (109 cases) in Chiba Cancer Center, Japan, from 2007 to 2009, 15 ALK fusion gene-positive NSCLC patients were initially screened by immunohistochemical procedures. Diagnoses were confirmed by RT-PCR and/or FISH for their molecular translocation.

2.1. ALK fusion protein detection by immunohistochemical methods

The intercalated antibody-enhanced polymer method of Takeuchi et al. [12,13] was used to detect ALK proteins. Formalin-fixed paraffin-embedded tissue was sliced at a thickness of 4 μm and the sections were placed on silane-coated slides. For antigen retrieval, the slides were heated for 40 min at 97 °C in target Retrieval Solution (pH 9.0; Dako). They were then incubated at room temperature, first with Protein Block Serum-free Ready-to-Use solution (Dako) for 10 min, and then with an anti-ALK antibody (5A4, Abcam) for 30 min. To increase the sensitivity of detection, we included an incubation step of 15 min at room temperature with rabbit polyclonal antibodies to mouse immunoglobulin (Dako). The immune complexes were then detected with the dextran polymer reagent and an AutoStainer instrument (Dako).

2.2. Confirmation of EML4-ALK fusion gene by RT-PCR and FISH

We confirmed the existence of ALK fusion gene expression by fluorescence in situ hybridization (FISH) and/or by the reverse transcription-polymerase chain reaction (RT-PCR).

2.3. Fluorescence in situ hybridization (FISH)

An EML4-ALK fusion assay was performed [10–12]. Unstained sections were processed with a Histology FISH Accessory Kit (Dako), subjected to hybridization with fluorescence-labeled bacterial artificial chromosome clone probes for EML4 and ALK (self-produced probes; EML4: RP11-996L7, ALK: RP11-984I21 and RP11-62B19), stained with 4,6-diamidino-2-phenylindole, and examined with a fluorescence microscope (BX51; Olympus). The FISH positivity criteria specified "over 50% cancer cells" for EBUS-TBNA samples.

2.4. Reverse transcription-polymerase chain reaction (RT-PCR)

The multiplex PCR method proposed by the Japanese ALK lung cancer study group (ALCAS) was used to confirm the expression of ALK fusion gene [4–6].

Table 1
Characteristics of ALK fusion gene positive lung cancer patients.

Patient no	Sex	Age	SI	Histology	Variant	p Stage	Therapy	Recurrence	Distant meta	Survival (M)	Prognosis	ALK inhibitor case no
1	f	64	0	Ad: papillary	3	IIIA	Surgery	Positive	Bone, brain	21	Dead	
2	m	82	0	Ad: solid	2	IIIA	Surgery	Positive	Ascites	36	Alive	
3	f	68	0	Ad: papillary	3	IIIB	Surgery	Positive	Brain	34	Alive	
4	f	60	0	Ad: solid	3	IIIA	Surgery	Negative	None	29	Alive	
5	m	73	0	Ad: acinar	3	IA	Surgery	Negative	None	21	Alive	
6	m	66	0	Ad: papillary	KIF5B	IA	Surgery	Negative	None	15	Alive	
7	m	56	300	Ad: papillary	1	IA	Surgery	Negative	None	13	Alive	
8	m	46	0	Ad: acinar	5	IIIA	Surgery	Negative	None	22	Alive	
9	m	71	0	Ad: papillary	1	IIIA	Surgery	Negative		17	Alive	
10	f	73	0	Ad: acinar	1	IV	Surgery	Negative		14	Alive	
11	m	55	100	Ad: muc+	3	IV	BSC		Bone, brain	5	Dead	
12	m	48	0	Ad: muc+	1	IV	Chemo		Bone, brain	29	Dead	Case 1
13	f	49	0	Ad: muc+	3	IV	BSC		Bone, brain	15	Alive	Case 2
14	f	54	0	Ad: muc+	1	IV	Chemo		Bone, brain, pul	22	Alive	Case 3
15	f	64	0	Ad: acinar	3	IV	Chemo		Pul	2	Alive	

SI, smoking index; f, female; m, male; Ad, adenocarcinoma; muc+, mucin production; Distant meta, at the recurrence (surgery group) at the diagnosis (non-surgery group); pul, pulmonary metastasis; Case 1 was already reported by Nakajima et al. [16].

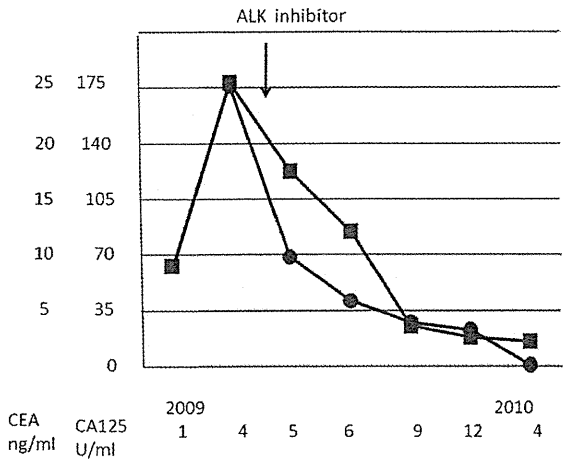

Fig. 1. Changes of tumor markers before and during the treatment with ALK inhibitor (Case 1) CEA (■), CA125 (●). Marked reduction of tumor markers was observed.

Total RNA was isolated from EBUS-TBNA or surgical samples using AllPrep DNA/RNA Mini Kit (Qiagen) and was reverse-transcribed into single strand cDNA using a High Capacity RNA-to-cDNA Kit (Applied Biosystems). To detect a fusion cDNA derived from EML4 or KIF5B and ALK, PCR analysis was performed with the AmpliTaq Gold PCR Master Mix (Applied Biosystems), the forward primers derived from EML4, EA-F-cDNA-S (5′-GTGCAGTGTTTAGCATTCTTGGGG-3′), EA-F-2-g-S (5′-AGCTACATCACACACCTTGACTGG-3′), EA-F-cDNA-v3-S-2 (5′-TACCAGTGCTGTCTCAATTGCAGG-3″) and EA-W-cDNA-in-S (5′-GCTTTCCCCGCAAGATGGACGG-3′) and the forward primers derived from KIF5B, KA-F-cDNA-S-e24 (5′-CAGCTGAGAGAGTGAAAGCTTTGG-3′), KA-F-cDNA-S-e17 (5′-GACAGTTGGAGGAATCTGTCGATG-3′), KA-F-cDNA-S-e11 (5′-ATCCTGCGGAACACTATTCAGTGG-3′), and KA-cDNA-S-e2 (5′-TCAAGCACATCTCAAGAGCAAGTG-3′) and the reverse primer derived from ALK, EA-F-cDNA-A (5′-TCTTGCCAGCAAAG-CAGTAGTTGG-3′). PCR products were purified from gel bands using QIAquick Gel Extraction Kit (Qiagen) and confirmed by direct sequencing analysis.

2.5. Enrolment of patients for the Clinical Trial A8081001

Informed consent was obtained from each patient to be enrolled for the study [10]. Eligibility criteria for the enrolment of ALK translocation positive patients into the ALK TKI PI Trial were as required by the Committee of Clinical Trials A8081001.

3. Results

There were 15 ALK fusion gene-positive cases which were screened immunohistochemically and confirmed by RT-PCR and FISH [14,15]. Eight patients were men and 7 women, of mean age

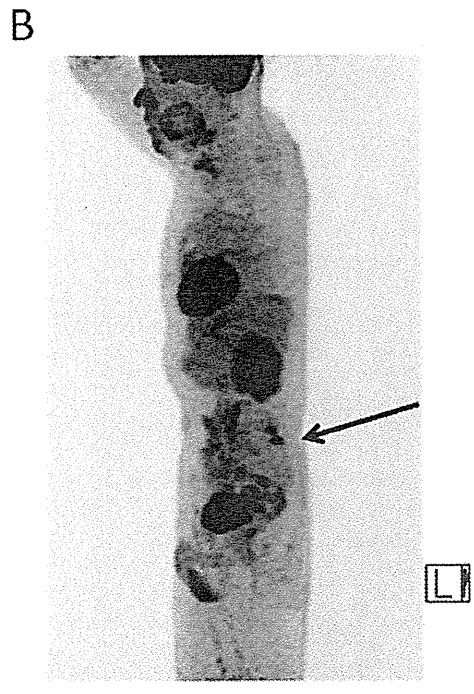

Fig. 2. FDG-PET scan of Case 1 performed at the same time (09/28/2009) as the previously reported Fig. 1D (Nakajima et al. [16]) shows bone metastasis of the left vertebral arch of L5 (arrow) in a sagittal view.

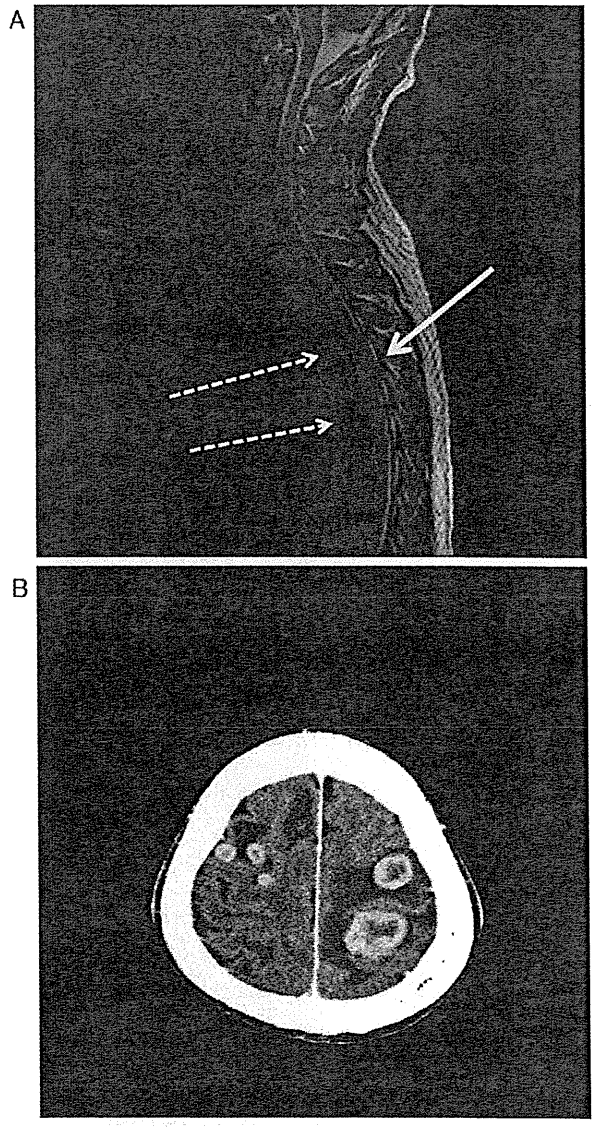

Fig. 3. MRI (Case 1) of the spinal cord on 04/05/2010 shows the metastases to the spinal cord (straight allow) and the spinal column (Th 4,6 dotted allow). B. CT scan (Case 1) of the brain on 04/05/2010 shows multiple brain metastases.

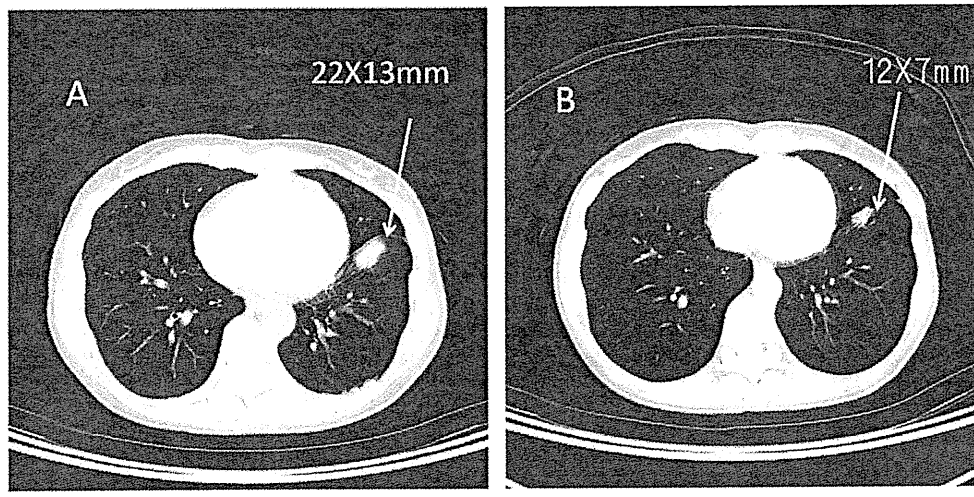

Fig. 4. CT scan (Case 2): A, 07/22/2009 (before ALK inhibitor) and B, 09/02/2009 (5 weeks after the initiation of the therapy). Left S8 tumor (arrow) decreased in size from 22X13 mm to 12X7 mm (PR).

61.9 years (range 48–82). Most were non-smokers, but 2 smoked lightly (Table 1). All tumors were adenocarcinomas with a papillary pattern predominant (5 cases), an acinar pattern predominant (3 cases), with mucin production (4 cases), etc. There were fourteen cases of fusion with EML4 and one KIF5B gene. There were 7 variant 3, 5 variant 1, and 1 each of variants 2 and 5. There were 3 stage IA, 5 stage IIIA, 1 stage IIIB and 6 stage IV cases. Ten cases were diagnosed after surgical resection, and 5, by tissue samples obtained with EBUS-TBNA. Ten cases underwent thoracotomy, 3 cases, chemotherapy, and 2 cases, only best supportive care. Of 5 cases diagnosed by EBUS-TBNA, 2 cases receiving chemotherapy and one receiving best supportive care were enrolled for the clinical trial. The mean age of the surgically treated group was 65.8 ± 10.1, and that of chemotherapy and BSC group was 54.0 ± 6.3. The difference was found by Student's t test to be statistically significant ($p < 0.05$), indicating that younger patients tend to have advanced cancer.

Out of 10 surgically treated cases, seven survived without a sign of recurrence, 3 had recurrence in both bone and brain tissue, and one died of bone and lymph node metastasis.

3.1. Case 1

Case 1 has already been reported in a case report (Nakajima et al.) [16] but without precise descriptions of the response to crizotinib, the adverse effects, the pattern of recurrence or the metastatic

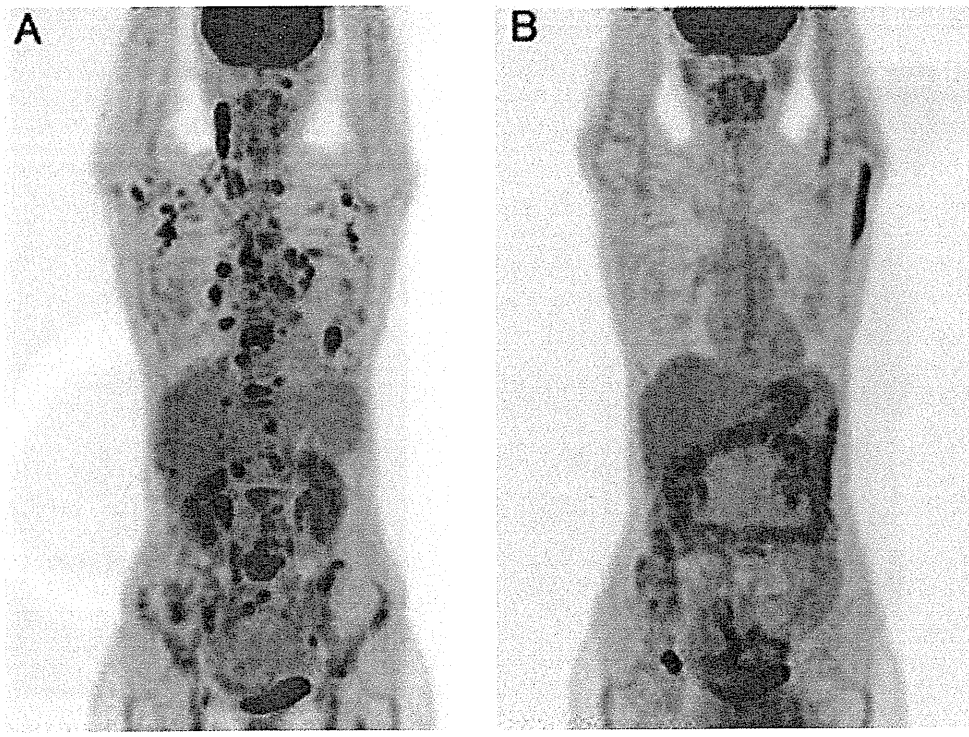

Fig. 5. FDG-PET scan (Case 2): A, 07/22/2009 (before ALK inhibitor) and B, 03/10/2010 FDG-PET scan shows marked reduction of accumulation in multiple bone and lymph node metastases 7 months after the initiation of the treatment.

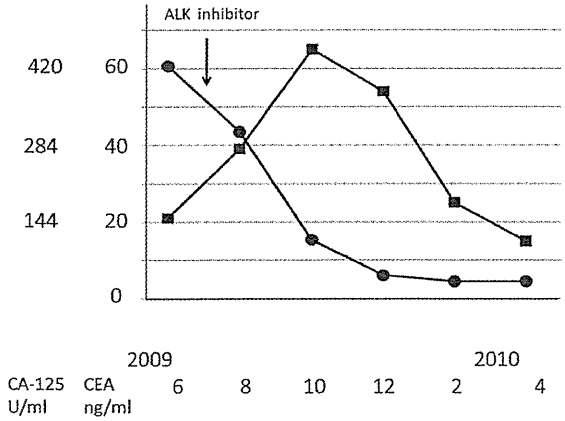

Fig. 6. Changes of tumor markers before and during the treatment with ALK inhibitor in case 2. CA125 (●) gradually decreased along with the treatment, but CEA (■) increased soon after the initiation of the therapy. The value of CEA then gradually decreased to 15.2 ng/ml in April 2010 (after 10 months).

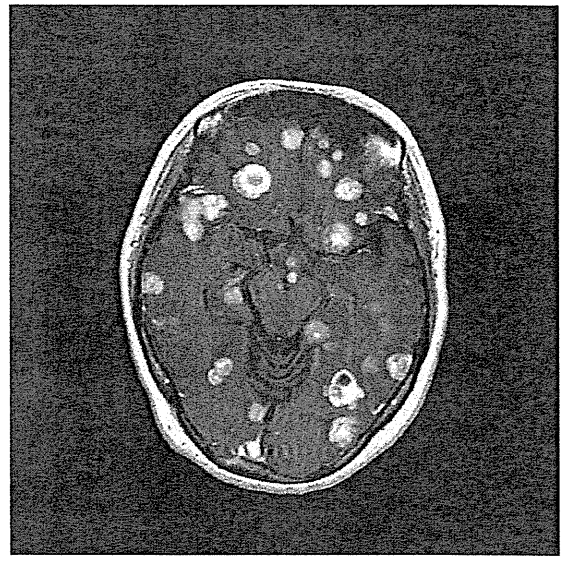

Fig. 7. Brain MRI of case 2 on 7/30/2010 showing multiple metastases.

tumor lesions. Such descriptions may contribute to a better understanding of the other cases, and so case 1 is described briefly below.

A 48-year-old non-smoking male patient had lung adenocarcinoma in the right lower lobe and multiple bone and lymph node metastases (T3N2M1 stage IV) at his first medical examination in November 2007. After several courses of chemotherapy, the patient was enrolled in a trial of crizotinib (PF02341066) from May 5th 2009 at Seoul National University, in which the drug was orally administered at 500 mg/day.

The effect of ALK inhibitor appeared rapidly. The patient's dyspnea improved within one week after drug administration. PS improved from 2 to 0 and a marked reduction in the tumor markers was observed (Fig. 1). Within 3 months after the start of therapy, almost all metastases disappeared except for those at the left vertebral arch of L5 (Fig. 2, arrow). The patient had severe adverse effects: diarrhea, nausea and persistence of light images started soon after the administration of the drug, but these gradually diminished over a 3-week period.

The control of the primary and metastatic tumors continued for 11 months until the patient visited Seoul University in April 2010, when he was hospitalized for paralysis of the lower extremities. MRI revealed spinal column (Th4-6) and spinal cord metastases (Fig. 3A). Soon after his hospitalization in our Cancer Center in April 2010, multiple brain metastases (Fig. 3B) were found, so the drug administration was stopped and he was transferred to a palliative care unit.

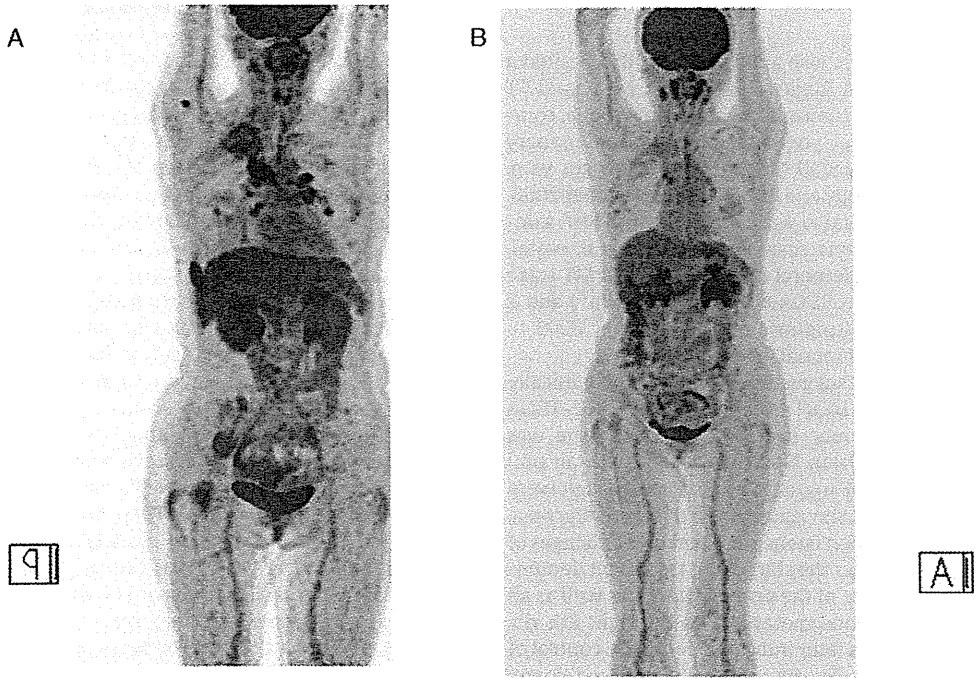

Fig. 8. FDG-PET scan: A, 09/08/2009 (before ALK inhibitor) and B, 07/05/2010 FDG-PET scan follow-up for 10 months indicated complete control of primary and distant metastases in case 3.